GRADO EN INGENIERÍA EN TECNOLOGÍAS INDUSTRIALES

TRABAJO FIN DE GRADO

EFFORTS TOWARDS THE STANDARDIZATION OF SUPERCONDUCTING CABLES

Autor: Martín-Sanz Garrido, Carmen

Director: Quéval, Loïc

Madrid

Declaro, bajo mi responsabilidad, que el Proyecto presentado con el título

EFFORTS TOWARDS THE STANDARDIZATION OF SUPERCONDUCTING CABLES

en la ETS de Ingeniería - ICAI de la Universidad Pontificia Comillas en el

curso académico 2021/21 es de mi autoría, original e inédito y

no ha sido presentado con anterioridad a otros efectos.

El Proyecto no es plagio de otro, ni total ni parcialmente y la información que ha sido

tomada de otros documentos está debidamente referenciada.

Fdo.: Carmen Martín-Sanz Garrido Fecha: 05/ 09/ 2021

Autorizada la entrega del proyecto

EL DIRECTOR DEL PROYECTO

Fdo.: Dr. Loïc Quéval Fecha: 05/ 09/ 2021

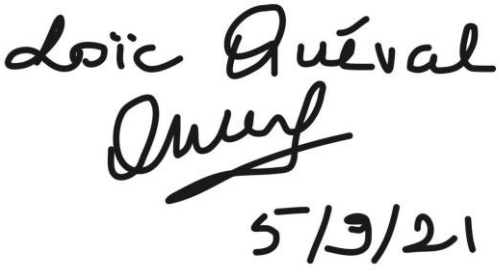

AUTORIZACIÓN PARA LA DIGITALIZACIÓN, DEPÓSITO Y DIVULGACIÓN EN RED DE PROYECTOS FIN DE GRADO, FIN DE MÁSTER, TESINAS O MEMORIAS DE BACHILLERATO

1º. Declaración de la autoría y acreditación de la misma.

El autor D. Carmen Martín-Sanz Garrido DECLARA ser el titular de los derechos de propiedad intelectual de la obra: EFFORTS TOWARDS THE STANDARDIZATION OF SUPERCONDUCTING CABLES, que ésta es una obra original, y que ostenta la condición de autor en el sentido que otorga la Ley de Propiedad Intelectual.

2º. Objeto y fines de la cesión.

Con el fin de dar la máxima difusión a la obra citada a través del Repositorio institucional de la Universidad, el autor **CEDE** a la Universidad Pontificia Comillas, de forma gratuita y no exclusiva, por el máximo plazo legal y con ámbito universal, los derechos de digitalización, de archivo, de reproducción, de distribución y de comunicación pública, incluido el derecho de puesta a disposición electrónica, tal y como se describen en la Ley de Propiedad Intelectual. El derecho de transformación se cede a los únicos efectos de lo dispuesto en la letra a) del apartado siguiente.

3º. Condiciones de la cesión y acceso

Sin perjuicio de la titularidad de la obra, que sigue correspondiendo a su autor, la cesión de derechos contemplada en esta licencia habilita para:

a) Transformarla con el fin de adaptarla a cualquier tecnología que permita incorporarla a internet y hacerla accesible; incorporar metadatos para realizar el registro de la obra e incorporar "marcas de agua" o cualquier otro sistema de seguridad o de protección.
b) Reproducirla en un soporte digital para su incorporación a una base de datos electrónica, incluyendo el derecho de reproducir y almacenar la obra en servidores, a los efectos de garantizar su seguridad, conservación y preservar el formato.
c) Comunicarla, por defecto, a través de un archivo institucional abierto, accesible de modo libre y gratuito a través de internet.
d) Cualquier otra forma de acceso (restringido, embargado, cerrado) deberá solicitarse expresamente y obedecer a causas justificadas.
e) Asignar por defecto a estos trabajos una licencia Creative Commons.
f) Asignar por defecto a estos trabajos un HANDLE (URL *persistente)*.

4º. Derechos del autor.

El autor, en tanto que titular de una obra tiene derecho a:

a) Que la Universidad identifique claramente su nombre como autor de la misma.
b) Comunicar y dar publicidad a la obra en la versión que ceda y en otras posteriores a través de cualquier medio.
c) Solicitar la retirada de la obra del repositorio por causa justificada.
d) Recibir notificación fehaciente de cualquier reclamación que puedan formular terceras personas en relación con la obra y, en particular, de reclamaciones relativas a los derechos de propiedad intelectual sobre ella.

5º. Deberes del autor.

El autor se compromete a:

a) Garantizar que el compromiso que adquiere mediante el presente escrito no infringe ningún derecho de terceros, ya sean de propiedad industrial, intelectual o cualquier otro.
b) Garantizar que el contenido de las obras no atenta contra los derechos al honor, a la intimidad y a la imagen de terceros.
c) Asumir toda reclamación o responsabilidad, incluyendo las indemnizaciones por daños, que pudieran ejercitarse contra la Universidad por terceros que vieran infringidos sus derechos e intereses a causa de la cesión.

d) Asumir la responsabilidad en el caso de que las instituciones fueran condenadas por infracción de derechos derivada de las obras objeto de la cesión.

6º. Fines y funcionamiento del Repositorio Institucional.

La obra se pondrá a disposición de los usuarios para que hagan de ella un uso justo y respetuoso con los derechos del autor, según lo permitido por la legislación aplicable, y con fines de estudio, investigación, o cualquier otro fin lícito. Con dicha finalidad, la Universidad asume los siguientes deberes y se reserva las siguientes facultades:

- La Universidad informará a los usuarios del archivo sobre los usos permitidos, y no garantiza ni asume responsabilidad alguna por otras formas en que los usuarios hagan un uso posterior de las obras no conforme con la legislación vigente. El uso posterior, más allá de la copia privada, requerirá que se cite la fuente y se reconozca la autoría, que no se obtenga beneficio comercial, y que no se realicen obras derivadas.
- La Universidad no revisará el contenido de las obras, que en todo caso permanecerá bajo la responsabilidad exclusive del autor y no estará obligada a ejercitar acciones legales en nombre del autor en el supuesto de infracciones a derechos de propiedad intelectual derivados del depósito y archivo de las obras. El autor renuncia a cualquier reclamación frente a la Universidad por las formas no ajustadas a la legislación vigente en que los usuarios hagan uso de las obras.
- La Universidad adoptará las medidas necesarias para la preservación de la obra en un futuro.
- La Universidad se reserva la facultad de retirar la obra, previa notificación al autor, en supuestos suficientemente justificados, o en caso de reclamaciones de terceros.

Madrid, a 05. De Septiembre de 2021

ACEPTA

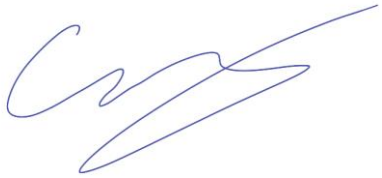

Fdo…Carmen Martín-Sanz Garrido

Motivos para solicitar el acceso restringido, cerrado o embargado del trabajo en el Repositorio Institucional:

GRADO EN INGENIERÍA EN TECNOLOGÍAS INDUSTRIALES

TRABAJO FIN DE GRADO

EFFORTS TOWARDS THE STANDARDIZATION OF SUPERCONDUCTING CABLES

Autor: Martín-Sanz Garrido, Carmen

Director: Queval, Loïc

Madrid

Acknowledgements

My deepest gratitude to my project supervisor, Dr. Loïc Quéval, for introducing me to the fascinating world of superconductivity and for guiding me through all the stages of this project during such a complicated academic year.

CONTRIBUCIÓN A LA ESTANDARIZACIÓN DE CABLES SUPERCONDUCTORES

Autor: Martin-Sanz Garrido, Carmen.
Director: Queval, Loïc.
Entidad Colaboradora: Université Paris-Saclay, GeePs

RESUMEN DEL PROYECTO

El fin de este proyecto es contribuir a la estandarización de los cables superconductores por dos vías: teórica y experimental. Se propone un marco de diseño multifísico de cables superconductores de corriente alterna para acelerar la fase su diseño. Adicionalmente, se ha construido en el laboratorio un banco de test para caracterizar cables superconductores.

Palabras clave: Cable, Test, Superconductor, Superconductividad, HTS

1. Introducción

La electrificación de muchos procesos y el auge de fuentes de energía renovables requiere de grandes interconexiones para poder transportar la electricidad en largas distancias minimizando pérdidas. La tecnología convencional de transporte de electricidad es el conductor resistivo, que conlleva pérdidas de efecto Joule, las cuales generan un impacto negativo tanto económica como medioambientalmente. Por ello, interesa encontrar una forma de reducir estas pérdidas.

En este contexto, el desarrollo de cables superconductores se convierte en una tarea clave ya que presentan una resistencia eléctrica nula y, por tanto, no generan pérdidas de efecto Joule.

A pesar de que los cables superconductores ya son tecnológicamente maduros, el número de implementaciones comerciales en la red es limitado debido a la falta de normas sobre diseño, construcción, puesta en marcha y funcionamiento. Por ello, la comunidad científica está implicada en los trabajos de normalización. La intención de este proyecto es unirse a dicho esfuerzo, contribuyendo a la caracterización de los cables superconductores tanto de manera teórica como experimental.

2. Definición del proyecto

El objetivo es contribuir hacia la estandarización de los cables superconductores por dos vías: teórica y experimental.

Múltiples cables superconductores han sido ya instalados en la red eléctrica, pero cada uno de ellos ha sido concebido de forma independiente y utiliza un modelo diferente, de ahí la falta de estandarización. El objetivo principal de este proyecto es contribuir a dicha estandarización, proponiendo un modelo multifísico de cables superconductores de corriente alterna que acelere su fase de diseño.

Además, se construye una instalación de pruebas para medir las propiedades de los núcleos de los cables. Dicha instalación se compone de un criostato, dos terminales y el dispositivo de medición necesario para poder medir dichas propiedades.

3. Descripción del modelo

El modelo de cable superconductor ha de definir completamente el comportamiento del mismo. Para ello, hay que seguir una metodología de diseño concreta, propuesta inicialmente en [NOE17]. La Ilustración 1 muestra la arquitectura de cable a diseñar

Ilustración 1 – Arquitectura de cable en configuración "1 fase 1 criostato", [NOE17]

El primer paso corresponde al modelo geométrico, que utiliza los requisitos y las limitaciones del diseño del cable, definiendo la posición y dimensiones de las distintas capas, tanto del núcleo como del criostato. El siguiente, es el modelo hidráulico que recibe la geometría del cable y calcula la presión a su salida para verificar que el rango de presión operacional es respetado.

A continuación, está el modelo térmico que determina la distribución de la temperatura tanto axial como radialmente, obteniendo el perfil de temperatura tridimensional del cable. Este modelo provee la temperatura en las capas superconductoras para luego calcular las pérdidas AC y, a la vez, permite controlar si en algún punto del cable se superan los límites de temperatura máxima o mínima de funcionamiento y, así, saber si la geometría propuesta es viable o no.

Finalmente, se aplica el modelo de pérdidas. Aunque en los cables superconductores no se producen pérdidas de efecto Joule, sí se producen pérdidas eléctricas (dieléctricas y AC) y térmicas debido al calentamiento del nitrógeno líquido. También hay que tener en cuenta las pérdidas generadas en los accesorios del sistema de cable superconductor como los terminales. Estas pérdidas no se pueden despreciar si quiere realizar un estudio de viabilidad técnica.

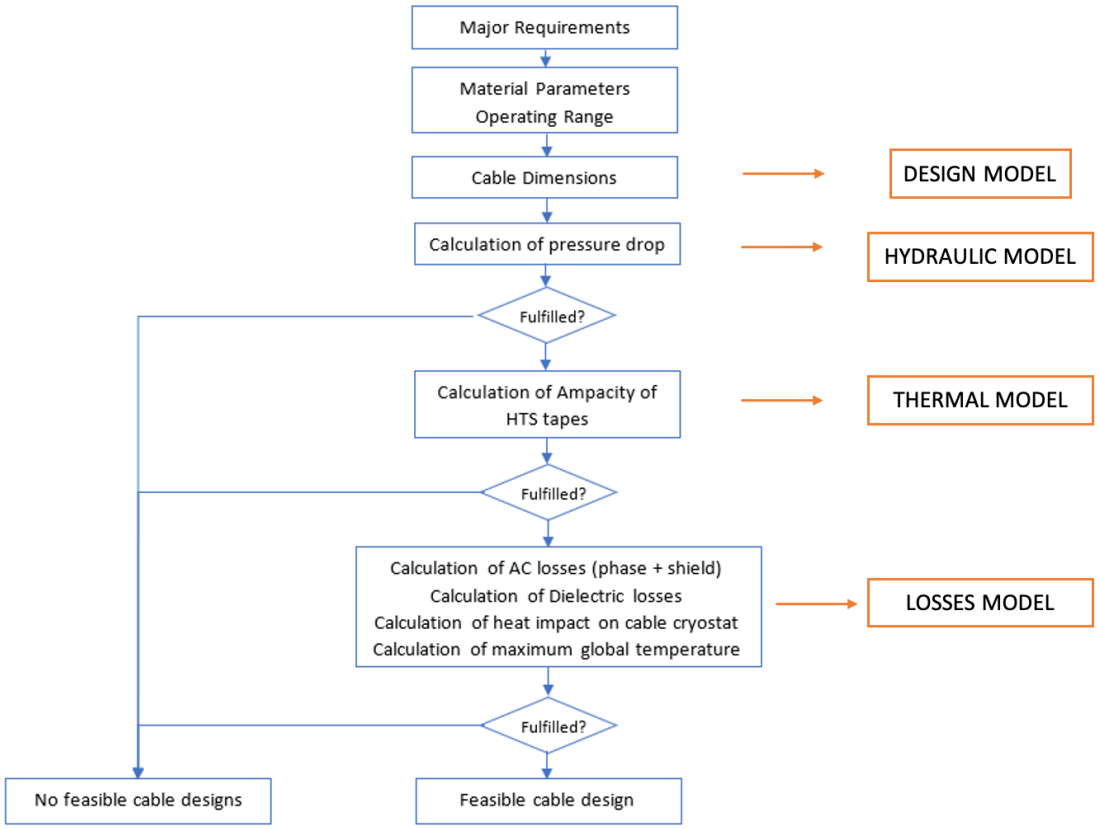

Ilustración 2 – Metodología de diseño propuesta para el simulador de cable superconductor

Cabe resaltar que los cables superconductores pueden disponerse en numerosas configuraciones (ver el estado de la técnica). El modelo multifísico propuesto en este proyecto sólo abarca seis de todas las configuraciones de cable posibles ya que el objetivo es mostrar la viabilidad del modelo. Mas adelante, el modelo podría ser expandido para abarcar un mayor número de configuraciones.

Tabla A – Configuraciones de cable abarcadas por el modelo multifísico

Configuración del cable	Tipo de Former	Diámetro de Former [mm]
1 fase 1 criostato	Hollow Conductor (HC)	DN 32
		DN 40
		DN 50
	Corrugated Tube (CT)	DN 32
		DN 40
		DN 50

En cuanto al aspecto experimental: se construye la estación de test a partir de dos protocolos, uno para la estandarización de la medida de la curva corriente-tensión en una cinta superconductora y, otro, para la soldadura de un núcleo de cable superconductor a un conector de cobre.

4. Resultados

Una vez creado el modelo de cable superconductor (por razones de confidencialidad, solo se incluye parte de dicho código Matlab en el Anexo I), para demostrar su utilidad, la segunda fase del proyecto ha sido aplicarlo al caso real presentado en [KOTT19]

Tabla B – Requisitos del cable a simular

Símbolo	Descripción	Valor	Unidad
Entrada			
L_{cable}	Longitud total del núcleo del cable	3200	m
U_n	Tensión Nominal [L-L, RMS]	380	kV
I_r	Corriente Nominal [L-N, RMS]	3600	A
$\dot{m}$	Flujo másico de nitrógeno liquido	0.9	kg/s
T_{in}	Temperatura del nitrógeno en la entrada del cable	68	K
P_{in}	Presión del nitrógeno en la entrada del cable	3	bar
Parámetros			
f	Frecuencia de la red	50	Hz
α_{drill}	Angulo de torsión de cinta superconductora	15	°
w_{tape}	Ancho de cinta superconductora	0.004	m
k_{SI}	Factor de seguridad	0.8	-
I_c	Corriente crítica de las cintas superconductoras	150	A
T_c	Temperatura crítica de las cintas superconductoras	90	K
T_0	Temperatura SF de las cintas superconductoras	77	K

De todas las configuraciones simuladas para los requisitos de la Tabla B, sólo dos de ellas fueron completadas, ya que, las demás, no cumplían los requisitos de presión establecidos. Las configuraciones posibles son las de diámetro de 50 mm (DN 50), tanto para el Corrugated Tube (CT), como el Hollow Conductor (HC). Las siguientes ilustraciones muestran la diferencia de resultados entre ambas configuraciones para los distintos submodelos:

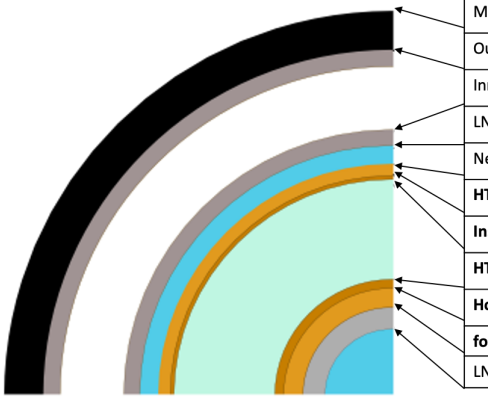

Layer	CT [m]	HC [m]
Mantel (OD)	0.1660	0.1660
Outer Cryostat (OD)	0.1560	0.1560
Inner Cryostat (OD)	0.1500	0.1500
LN2 OUT (OD)	0.1320	0.1320
Neutral Conductor (OD)	0.1250	0.1250
HTS Shield (OD)	**0.1060**	**0.1107**
Insulation (OD)	**0.1020**	**0.1067**
HTS Conductor (OD)	**0.1016**	**0.1063**
Hollow Conductor (OD)	**0.0536**	**0.0578**
former (OD)	**0.0528**	**0.0574**
LN2 IN (OD)	0.0500	0.0500

Ilustración 3 – Geometría en diámetros exteriores de DN 50 Hollow Conductor vs Corrugated Tube

Una vez son especificados los requisitos de la tabla B, el modelo informático puede comenzar a trabajar. Como se ha explicado en la metodología, el primer submodelo es el geométrico, que proporciona la arquitectura interna del núcleo del cable y el criostato. La Ilustración 3 muestra la distribución y los diámetros externos de cada capa para las dos configuraciones viables: DN 50 CT y DN 50 HC.

Tabla C – Comparación de cantidad de material superconductor DN 50 CT vs HC

Configuración de cable	Capa cinta HTS	No. cintas HTS por capa	Espesor de capa [m]	Longitud total de cinta HTS [km]	Longitud de cinta por km de cable [m]
CT DN 50	Capa 1	40	0.002	265.03	82.82
	Capa 2	40	0.002		
HC DN 50	Capa 1	43	0.002	142.45	44.53

En la Ilustración 3 se aprecia que la elección del tipo de Former influye en la distribución de capas, aunque el diámetro de éste sea el mismo. Además, como se puede ver en la Tabla C, la diferencia en la distribución geométrica de las capas influye también en el número de capas de material superconductor y, por tanto, en la cantidad de material superconductor utilizado en la configuración.

Una vez que el diseño geométrico ha finalizado, el modelo hidráulico calcula el perfil de presión del nitrógeno líquido a lo largo del cable. En este caso, como ambos tipos de Former son modelados como una tubería lisa, se obtiene el perfil de presión de la Ilustración 4 para ambas configuraciones.

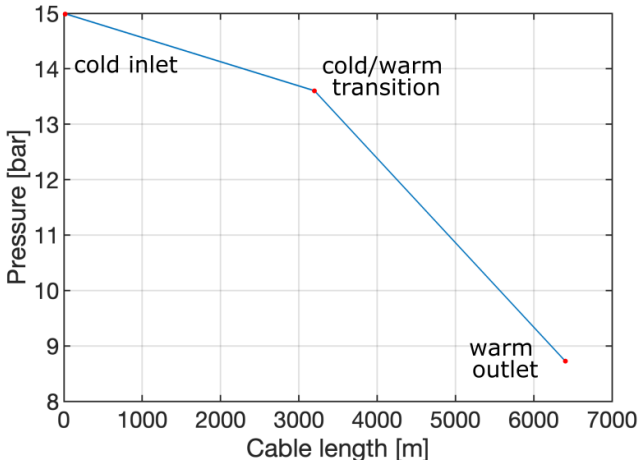

Ilustración 4 – Perfil de presión longitudinal del cable DN 50

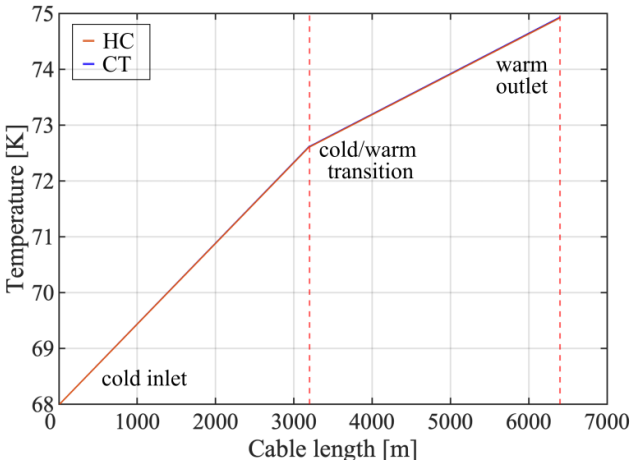

Ilustración 5 – Perfil longitudinal de temperatura del cable DN 50 CT vs HC

La Ilustración 4 verifica que los límites de presión operacional son respetados por lo que se puede proceder al modelo térmico para obtener el perfil de temperatura. La Ilustración 5 demuestra que las distintas cantidades de cintas HTS de cada configuración van a influir en

el perfil de temperatura del cable. Esto se debe a que, a mayor número de cintas (como es el caso de DN 50 HC)), menor cantidad de corriente por cada una de ellas, por lo que se reducen las pérdidas AC y, consecuentemente, menor temperatura.

Ya obtenido el perfil de temperatura, se utiliza el modelo de pérdidas. La Ilustración 6 confirma que, para un mismo diámetro, todas las pérdidas son iguales, independientemente de la configuración, excepto las pérdidas AC que, como se ha explicado ya, dependen directamente de la cantidad de cintas HTS de la geometría.

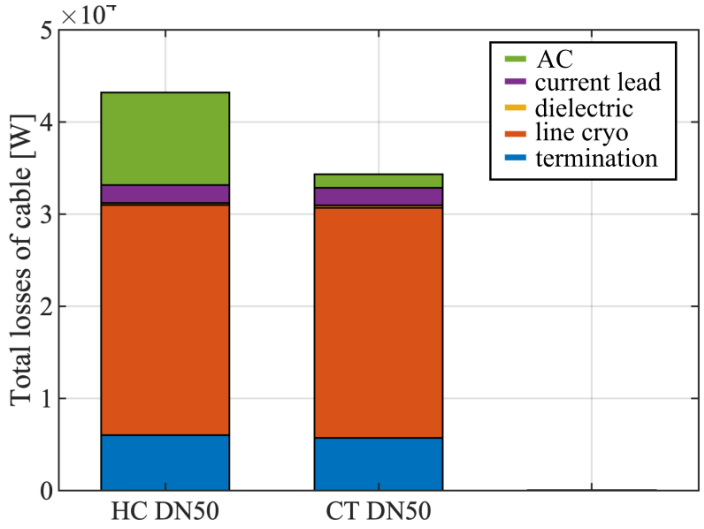

Ilustración 6 – Pérdidas totales cable DN 50 Hollow Conductor vs Corrugated Tube

En cuanto a la parte experimental, la Ilustración 7 muestra el resultado de la aplicación del protocolo de medida de IV para una cinta superconductora y, la Ilustración 8, el estado actual del banco de test (Para mas detalles consultar Capitulo 7).

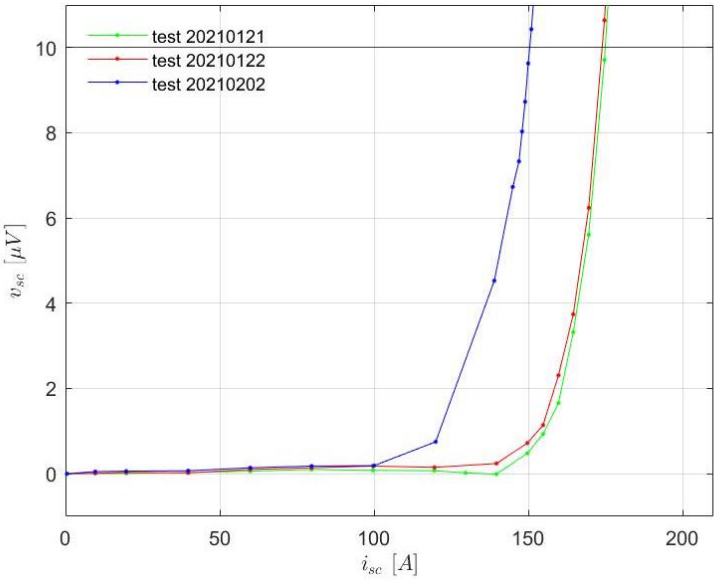

Ilustración 7 – Resultado de la medida IV de una cinta superconductora

Ilustración 8 – Estado actual del banco de prueba

5. Conclusiones

El objetivo de este proyecto es contribuir a la estandarización de los cables superconductores. A lo largo del desarrollo del proyecto se ha creado un marco para el diseño de un sistema de cables superconductores. Aunque el marco aún no cubre todas las posibilidades de configuraciones de cables HTS, su aplicación a la configuración de "1 núcleo 1 criostato" ha permitido obtener resultados que se verifican con trabajos anteriores. Este modelo no sólo ha servido para reproducir el comportamiento del cable superconductor sino que, también, permite comparar distintas configuraciones y, así, poder elegir la óptima en cada caso. Además, el modelo actual podría ampliarse fácilmente para cubrir más posibilidades y utilizarse dentro de una rutina de optimización.

En el aspecto experimental, se ha desarrollado un protocolo para estandarizar la medición de la característica I-V de una cinta superconductora. El uso de este protocolo puede unificar los resultados de diferentes pruebas y fabricantes, proporcionando una forma más fiable y precisa de comparar los resultados entre diferentes experimentos. Por último, la construcción de una estación de prueba de cables superconductores participa en el desarrollo de equipos de prueba avanzados en el laboratorio GeePs, ya que permitirá medir las propiedades de los cables superconductores sin depender de instalaciones de terceros y, por tanto, supondrá un paso adelante en el análisis y desarrollo de los cables superconductores.

6. Referencias

[NOE17] Noé, M. *Superconducting Cable. EUCAS Short Course Power Applications*, Geneva, 2017.

[KOTT19] Kottonau, D.; Shabagin, E.; de Sousa, W. *Evaluation of the Use of Superconducting 380 kV Cable*. KIT Scientific Publishing, 2019.

EFFORTS TOWARDS THE STANDARIZATION OF SUPERCONDUCTING CABLES

Author: Martín-Sanz Garrido, Carmen.
Supervisor: Queval, Loïc.
Collaborating Entity: Université Paris-Saclay, GeePs

ABSTRACT

The main objective of this project is to contribute to the standardization of superconducting cables. To do so, a framework for the multiphysics design of superconducting AC cable is proposed to speed up the design phase of a superconducting cable by creating a model that characterizes any HTS cable system. Additionally, a test bench has been built in the laboratory to characterize superconducting cables.

Keywords: Cable, Test, Superconductor, Superconductivity, HTS.

1. Introduction

The electrification of many processes and the rise of renewable energy sources require large interconnections to transport electricity over long distances while minimizing losses. The conventional technology for electricity transport is the resistive conductor, which involves Joule losses, creating a negative impact both economically and environmentally. It is therefore of interest to find a way to reduce these losses.

In this context, the development of superconducting cables becomes a key task since they have zero electrical resistance and therefore do not generate Joule losses.

Although superconducting cables are already technologically mature, the number of commercial implementations in the grid is limited due to the lack of standards on design, construction, commissioning, and operation. Therefore, the scientific community is involved in standardization work. The intention of this project is to join that effort, contributing to the characterization of superconducting cables both theoretically and experimentally

2. Project Objectives

The objective is to contribute towards the standardization of superconductor cables in two ways: theoretically and experimentally.

Multiple superconductor cables have already been installed in the power grid, but each of them has been conceived independently and uses a different model, hence the lack of standardization. The main objective of this project is to contribute to such standardization by proposing a framework for the multiphysics design of alternating current superconductor cables to accelerate their design phase.

In addition, a test facility is built to measure the properties of the cable cores. This installation consists of a cryostat, two terminals and the necessary measuring devices to measure these properties.

3. Description of the model

The superconducting cable model has to fully define the behavior of the superconducting cable. For this purpose, a specific design methodology, initially proposed in [NOE17], must be followed. Figure 1 shows the cable architecture to be designed.

Figure 4 – "1 phase 1 cryostat" HTS cable architecture, [NOE17]

The first step corresponds to the geometrical model, which uses the specification and limitations of the cable design and defines the position and dimensions of the different layers for both the core and the cryostat. Next comes is the hydraulic model, which receives the cable geometry and calculates the pressure at its outlet to verify that the operating pressure range is respected.

Next is the thermal model that determines the temperature distribution both axially and radially and provides the three-dimensional temperature profile of the cable. This model provides the temperature in the superconducting layers to then calculate the AC losses and, at the same time, allows to control if at any point of the cable the maximum or minimum operating temperature limits are exceeded and, thus, to know if the proposed geometry is feasible or not.

Finally, the loss model is applied. Although Joule effect losses do not occur in superconducting cables, electrical (dielectric and AC) and thermal losses do occur due to the heating of liquid nitrogen. Losses generated in the superconducting cable system accessories such as terminals must also be considered. These losses cannot be neglected if a technical viability study is to be made.

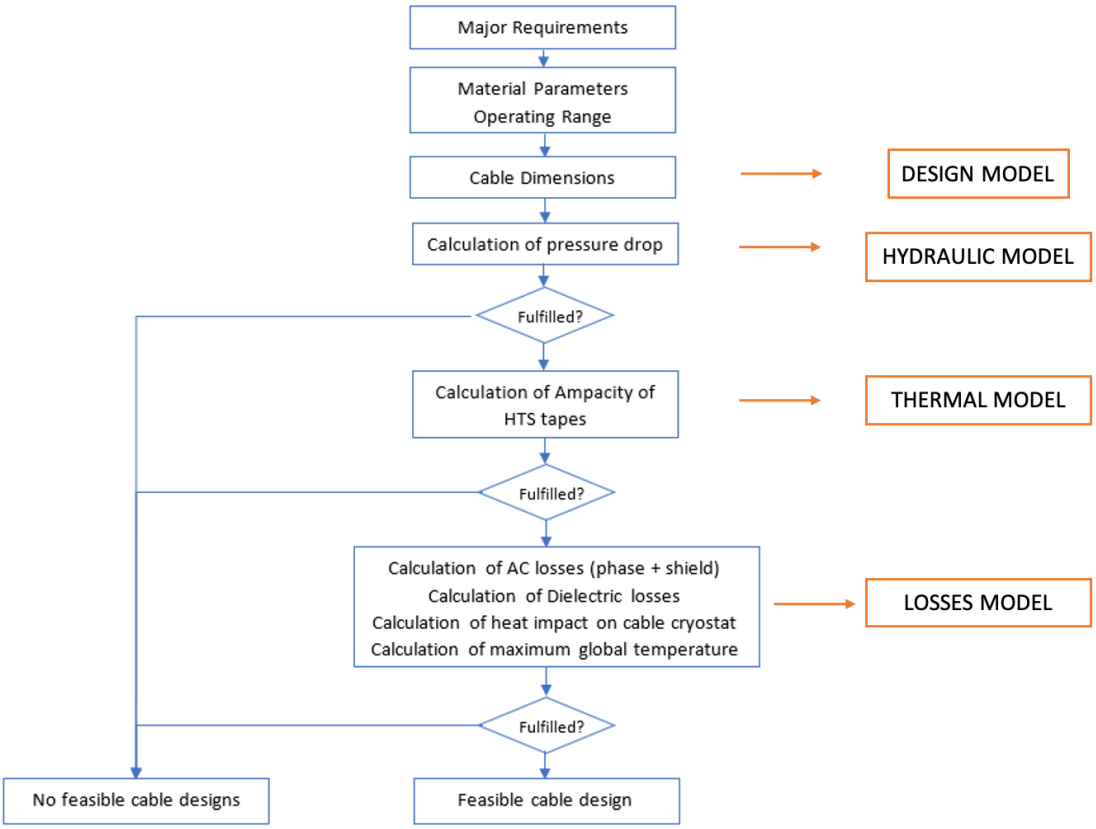

Figure 2 – Proposed design methodology

It should be noted that superconducting cables can be arranged in numerous configurations (see the state of the art). The multiphysics model proposed in this project only covers six of all possible cable configurations as the objective is to show the feasibility of the model. Later, the model could be expanded to cover a larger number of configurations.

Table A – Possible cable configurations studied in the work

Cable Configuration	Former Type	Former Diameter [mm]
1 phase 1 cryostat	Hollow Conductor (HC)	DN 32
		DN 40
		DN 50
	Corrugated Tube (CT)	DN 32
		DN 40
		DN 50

Regarding the experimental aspect: the test station is built based on two protocols, one for the standardization of the measurement of the I-V curve on a superconducting tape and the other for the soldering of a superconducting cable core to a copper connector.

4. Results

Once the superconducting cable model was created (part of the Matlab code provided in Annex I) to demonstrate its use, the second phase of the project was to apply it to the real case presented in [KOTT19].

Table B – Specifications of cable to reproduce

Symbol	Description	Value	Unit
Entrada			
L_{cable}	Total length of cable core	3200	m
U_n	Nominal Voltage [L-L, RMS]	380	kV
I_r	Nominal current [L-N, RMS]	3600	A
$\dot{m}$	LN2 mass flow	0.9	kg/s
T_{in}	Temperature of LN2 at cable inlet	68	K
P_{in}	Pressure of LN2 at cable inlet	3	bar
Parameters			
f	Network frequency	50	Hz
α_{drill}	Twist angle of tape	15	°
w_{tape}	HTS tape width	0.004	m
k_{SI}	Load factor	0.8	-
I_c	Critical current of HTS tapes	150	A
T_c	Critical temperature of HTS tapes	90	K
T_0	SF temperature of HTS tapes	77	K

Of all the configurations simulated for the requirements of Table B, only two of them were completed, as the others did not meet the pressure requirements. The possible configurations are 50 mm diameter (DN 50) for both Corrugated Tube (CT) and Hollow Conductor (HC). The following figures show the difference in results between the two configurations for the different submodels:

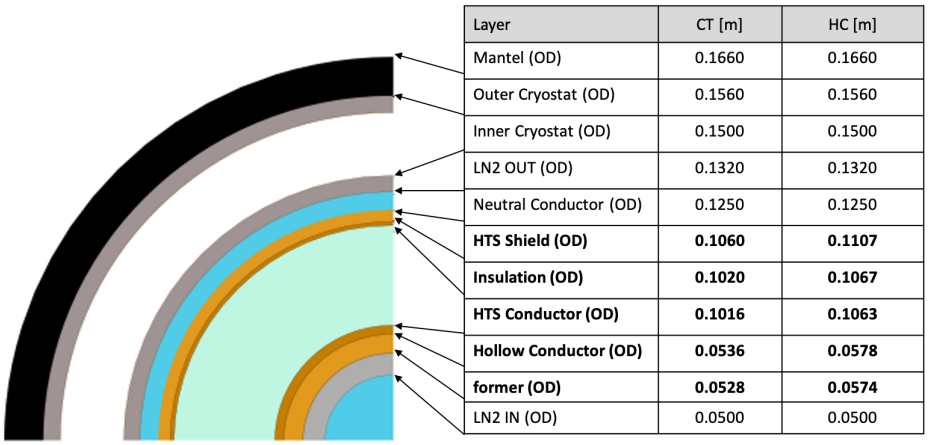

Figure 3 – Outer diameter geometry of DN 50 Hollow Conductor vs Corrugated Tube

Once the requirements of table B are specified, the computer model can start working. As explained in the methodology, the first submodel is the layout one, which provides the internal architecture of the cable core and cryostat. Figure 3 shows the distribution and external diameters of each layer for the two feasible configurations: DN 50 CT and DN 50 HC.

Table C – HTS tape quantity comparison DN 50 CT vs HC

Cable configuration	HTS tape layer	No. Tapes per layer	Layer thickness [m]	Total length of HTS tape [km]	Length of HTS tape per km of cable [m]
CT DN 50	Layer 1	40	0.002	265.03	82.82
	Layer 2	40	0.002		
HC DN 50	Layer 1	43	0.002	142.45	44.53

Figure 3 shows that the choice of Former type influences the distribution of layers, even if the diameter of the Former is the same. Furthermore, as can be seen in Table C, the difference in the geometrical distribution of the layers also influences the number of layers of superconducting material and, therefore, the amount of superconducting material used in the configuration.

Once the geometric design has been finalized, the hydraulic model calculates the pressure profile of the liquid nitrogen along the cable. In this case, as both former types are modeled as a smooth pipe, the following pressure profile (Figure 4) is obtained for both configurations.

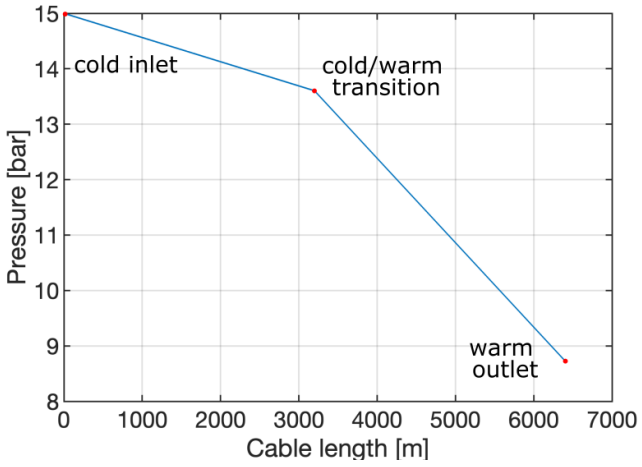

Figure 4 – Longitudinal pressure profile of cable DN 50

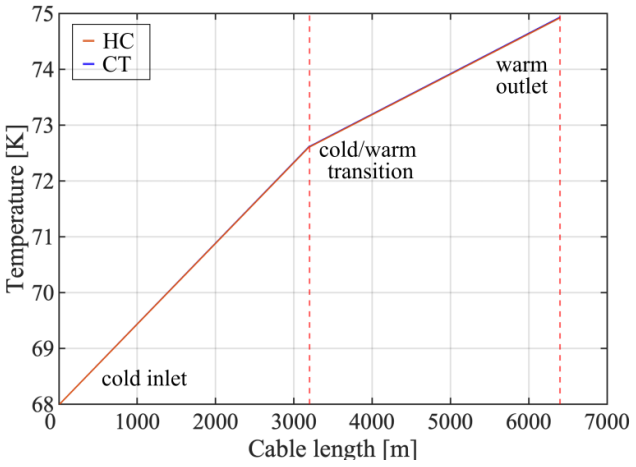

Figure 5 – Longitudinal temperature profile of cable DN 50 CT vs HC

Figure 4 verifies that the operational pressure limits are respected so that the thermal model can be run to obtain the temperature profile. Figure 5 shows that the different number of HTS tapes in each configuration will influence the temperature profile of the cable. This is since the higher the number of tapes (as in the case for DN 50 HC), the lower the amount of current per tape, thus reducing AC losses and, consequently, the lower the temperature.

Once the temperature profile has been obtained, the loss model is used. Figure 6 confirms that, for the same diameter, all the losses are the same, regardless of the configuration, except for the AC losses which, as already explained, depend directly on the number of HTS tapes in the geometry.

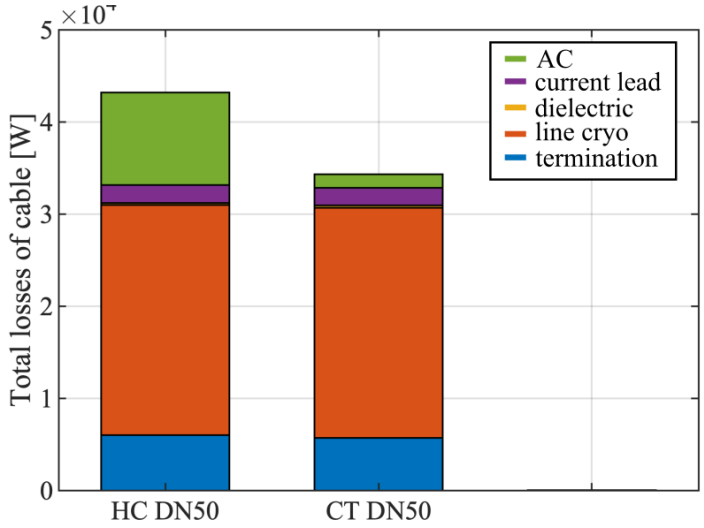

Figure 6 – Total losses of cable DN 50 Hollow Conductor vs Corrugated Tube

As for the experimental part, Figure 7 shows the result of the application of the I-V measurement protocol for a superconducting tape and Figure 8, the current status of the test bench (For more details see Chapter 7).

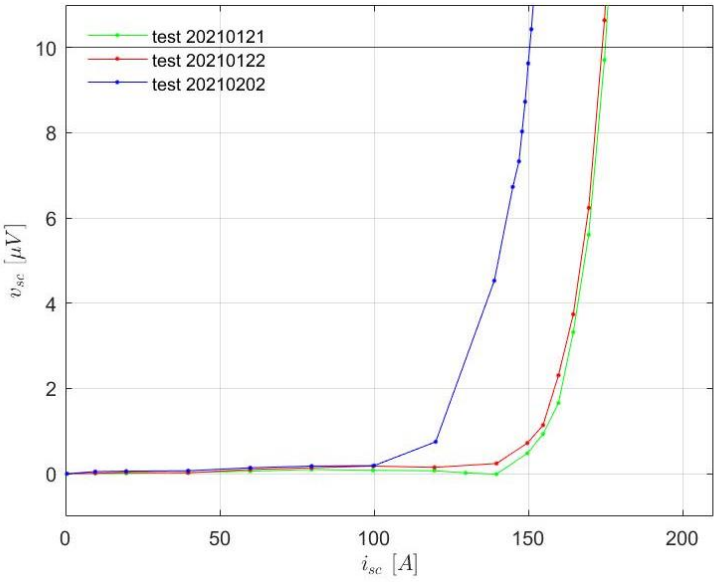

Figure 7 – Result of the measure I-V of a Sumitiomo_BSCCO_HTCA_CETS_2019_068_001 tape

Figure 8– Actual state of the test station

5. Conclusion

The objective of this project is to contribute to the standardization of superconducting cables.

Throughout the development of the project, a framework for the design of a superconducting cable system has been created. Although the framework does not yet cover all the possibilities of HTS cable configurations, its application to the "1 core 1 cryostat" configuration has yielded results that are verified with previous work. This model not only serves to reproduce the behavior of the superconducting cable, but also to compare different configurations and, thus, to choose the optimal one in each case. In addition, the current model could be easily extended to cover more possibilities and used within an optimization routine.

On the experimental side, a protocol has been developed to standardize the measurement of the I-V characteristic of a superconducting tape. The use of this protocol can unify results from different tests and manufacturers, providing a more reliable and accurate way to compare results between different experiments. Finally, the construction of a superconducting cable test station participates in the development of advanced test equipment in the GeePs laboratory, as it will allow the properties of superconducting wires to be measured without relying on third-party facilities and will therefore be a step forward in the analysis and development of superconducting wires.

6. References

[NOE17] Noé, M. *Superconducting Cable. EUCAS Short Course Power Applications*, Geneva, 2017.

[KOTT19] Kottonau, D.; Shabagin, E.; de Sousa, W. *Evaluation of the Use of Superconducting 380 kV Cable*. KIT Scientific Publishing, 2019.

Table of Contents

FIGURE INDEX

Chapter 1

Chapter 2

Chapter 3

Chapter 4

Chapter 5

Chapter 6

Chapter 7

TABLE INDEX

Chapter 1

Chapter 2

Chapter 3

Chapter 4

Chapter 5

Chapter 6

Chapter 7

CHAPTER 1 - INTRODUCTION

The electrification of many processes increases the need for electricity transport. Moreover, the diversification of the electricity sources with renewable energies implies to develop large interconnections. In this context, being able to transport electricity on very long distances with as few losses as possible is essential.

The conventional technology to transmit electricity is the resistive conductor, that has Joule losses. RTE, France's transmission system operator, states that Joule losses is responsible for 6 % of the national network's losses, amounting to 20 TWh/ [CDEN14] These losses affect the efficiency of the network and derive in both economic and environmental issues: economic because the loss energy is paid by the consumer but never received, and environmental because the existence of losses implies more production of energy to deliver less power, thus leading to more use of fossil fuels and non-renewable energy production processes.

In regard of this issue, it is in the interest of transmission system operators to find a way of reducing these losses. Moreover, the 193 member States of the United Nations agreed in 2015 on the Sustainable Development Goals, 17 goals interlinked with each other that set the "blueprint to achieve a better and sustainable future for all". Among these 17 goals, there are two which concern the issue of line losses: goal 7 and goal 9. Goal 7 sets the target of a cleaner energy sector, something that could be achieved through the elimination of Joule losses. Goal 9 sets the target of making more efficient and sustainable all industries and infrastructures. Again, eliminating Joule losses would be a key advancement to make the electric network, one of the biggest infrastructures of the world more efficient, as well as making the energy industry greener.

In this context, the development of superconducting cables becomes a key task. Indeed, a superconducting cable presents zero electrical resistance and therefore no Joule losses. This technology is also well suited for a high current density, compact, and lightweight applications. In addition, superconducting cables allow high transmission power using low voltage and reduced cable diameter. Moreover, with no Joule losses being generated, it would heat the ground less, which impacts less the environment.

However, for the proper operation of such cable, it is mandatory to keep them at cryogenic temperature. To do so, a cryogenic system is used to cool the cable and both its temperature and pressure must be controlled for the cable to remain in its superconducting state.

Superconducting cables are now technologically mature (see section 2.2.2) and cost-competitive for some applications [MERS13]. But, despite numerous research projects, the number of commercial grid implementations is limited. One of the main reasons for this is the lack of standards regarding the design, construction, commissioning, and operation of superconducting cable systems. Indeed, without standards, transmission system operators are unlikely to adopt the technology. Therefore, the community is now strongly involved in standardization work.

The aim of this work is to contribute to the efforts towards the standardization of superconducting cables, by carrying both theoretical and experimental work:

(i) On the theoretical side, we are laying down a framework to design AC superconducting cables.
(ii) On the experimental side, a superconducting cable test bench is being developed in the GeePs laboratory to allow in-house measurements and testing of superconducting cable.

Throughout chapters 3 to 4 of this report, the establishment of a framework to design AC superconducting cables will be detailed and implemented. Then, the model will be used to discuss some aspects of superconducting cable design.

In the chapter 7 of the report, the effort to develop the test station as well as the measurement protocol will be detailed. Explaining the necessity and fabrication of all components needed to perform an I-V test on a superconducting cable core.

CHAPTER 2 – STATE OF THE ART

The scientific community has been making efforts to develop superconducting cables and to make them cost-competitive during the past decades. In this section, the existing cable technologies using High Temperature Superconductors (HTS) will be summarized, as well as the superconducting cables that have been already commissioned.

Although both AC and DC superconducting cables exist, the current work focuses on AC cables. Nowadays, two types of configurations are used: cold and warm dielectric.

2.1 WARM DIELECTRIC

For the warm dielectric configuration, the outer dielectric insulation, the cable screen, and the outer cable sheath are at room temperature and outside the cryostat (Figure 2.1).

Figure 2. 1: Warm dielectric HTS cable [SCHM05]

Compared to conventional cables, this design offers a high-power density using the least amount of HTS-wire for a given level of power transfer.

2.2 COLD DIELECTRIC

For the cold dielectric configuration, the dielectric layer is inside the cryostat. A superconducting shield layer can be used. Three main cable architectures are used:

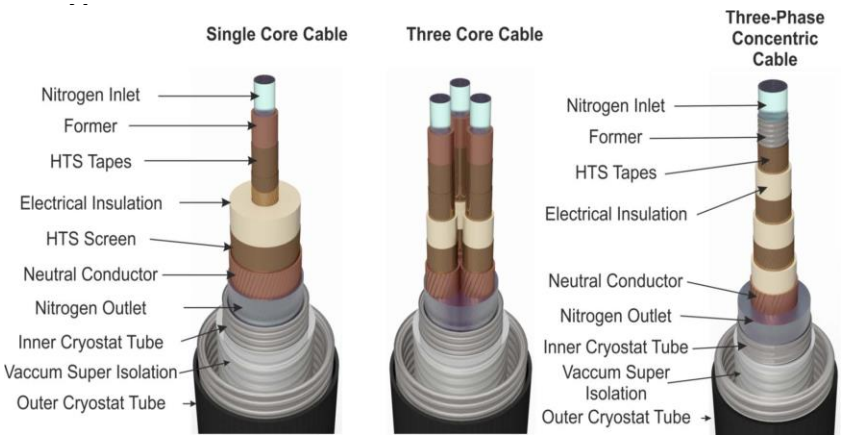

Figure 2. 2: Available cold dielectric cable architectures

- **1 phase 1 cryostat**, also called single core cable. This configuration is normally used in multiples of 3 to obtain a 3-phase system. In comparison with other configurations, it is the one that requires the most superconducting material and thus, the one that incurs in the most AC losses [NOE17]. On the other hand, it is the configuration with the highest voltage levels, up to 110 kV when 3 separate phases are used.
- **3 phase 1 cryostat**, also called three core cable. It consists of a single line cryostat housing three cable cores. This configuration allows for a small diameter for each of the cores and thus a reduced amount of superconducting material in each phase. Therefore, the configuration is used for cables with lower voltage: form 30 kV to 100 kV. However, each core needs its own shield, so it still uses a great amount of HTS material.
- **3 phase concentric.** The three phases of the cable are built one on top of the other and housed in the same cryostat. This configuration presents the least superconducting material out of all the col dielectric types. But its application is limited to low voltage applications: from 10 kV to 50 kV.

2.2.1 DEMONSTRATION CABLES

The process from conception to grid implementation can take many years. One intermediary step is to measure the cable properties in a testing facility. Figures 2.3 and 2.4 provide a graphic representation of Table 2.1.

Table 2. 1: Laboratory tested AC superconducting cables

Location, Manufacturer/Project	Year	Length	Material	Configuration	V, I (L-N RMS)	Operation Temperature	Ref.
Yokosuka, CRIEPI	2004	500 m	BSCCO	1 phase 1 cryostat	77 kV, 1 kA	73 K	[MUKO17][ICHI07]
Gochang, KEPCO	2006	100 m	BSCCO	3 phase 1 cryostat	22.9 kV, 1.25 kA	64 – 77 K	[HYUN09]
Hannover, Nexans	2007	30 m	YBCO	?	130 kV, 1.8 kA	?	[NOE_13]
Super3C, Nexans	2008	30 m	YBCO	1 phase 1 cryostat	10 kV, 1 kA	70 K	[TIXA10]
Moscow, Russian R&D	2009	30 m	BSCCO	1 phase 1 cryostat	20 kV, 2 kA	77 K	[SYNT09]
Weschester Country, Southwire	2010	25 m	?	3 phase concentric	13,8 kV, 4 kA	73 – 78 K	[MAGU10]
Amsterdam, Ultera	2010	6000 m	YBCO	3 phase 1 cryostat	50 kV, 2.9 kA	70 K	[MELN09]
Barcelona, ENDESA	2011	30 m	BSCCO	1 phase 1 cryostat	25 kV, 3.2 kA	65 – 70 K	[RAIN11]
Seoul, CAST	2011	400 m	YBCO	?	2.52 kV, 2.9 kA	?	[YOUN07]
St. Petersbourg, FGC UES	2015	2500 m	?	3 phase concentric	20 kV, 2.5 kA	68 – 78 K	[SYNT15]

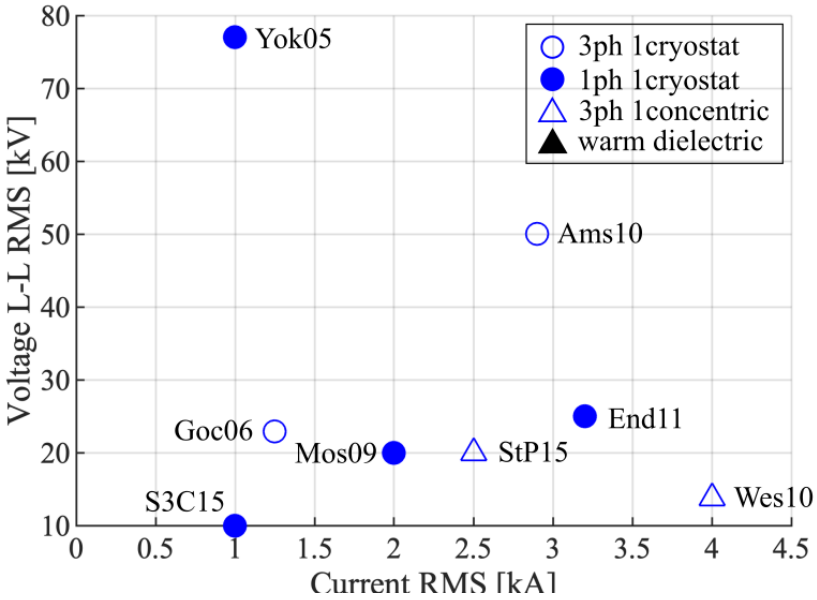

Figure 2. 3: I-V map of demonstrated AC HTS cables

The cable length ranges from several meters up to 6 km. Three phases concentric configuration is implemented only for low nominal voltages, not exceeding 20 kV., For applications with the highest nominal voltage (Yok05), the 1 phase 1 cryostat configuration was selected.

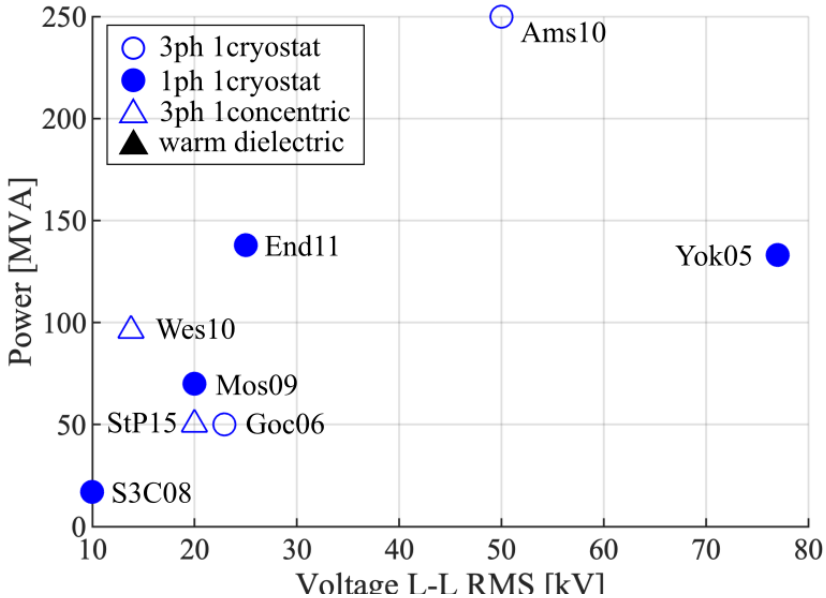

Figure 2. 4: P-V map of demonstrated AC HTS cables

2.2.2 COMMISSIONED CABLES

As shown in Table 2.2, several superconducting cables have already been successfully tested on the grid. The cable with the longest continuous operating time without interruption was

commissioned in Essen in April 2014, having a length of 1 km, a voltage of 10 kV and a power 40 MVA.

Table 2. 2: AC superconducting cables operating on the grid

Location, Manufacturer/Project	Commissioning	Length	Material	Configuration	V, I (L-N, RMS)	Operation Temperature	Ref
Carrolton, Southwire C.	2001	30 m	PIT-BSCCO	3 phase 1 cryostat	12.4 kV, 1.25 kA	70 – 80 K	[STOV11]
Copenhagen, C. Energy	2001	30 m	BSCCO	1 phase 1 cryostat	36 kV, 2 kA	79 – 82 K	[WILL02][TONE04]
Yunan, China Southern Grid	2004	30 m	BSCCO	Warm dielectric (1 phase 1 cryostat)	35 kV, 2 kA	70 – 76 K	[YXIN04]
Columbus, Ultera	2006	200 m	BSCCO	3 phase concentric	13,2 kV, 3 kA	77.6 K	[DEMK06][LINS08]
Albany, NY HTS	2006	350 m	DI-BSCCO	3 phase 1 cryostat	34.5 kV, 0.8 kA	69 – 73 K	[YUMU09]
Long Island, LIPA Grid I	2008	600 m	BSCCO	1 phase 1 cryostat	138 kV, 2.4kA	77 K	[SCHM12]
Icheon, LS Cable	2010	410 m	REBCO	3 phase 1 cryostat	22.9 kV, 1.25 kA	68.8 K	[SOHN12][CHEO13]
Long Island, LIPA Grid II	2011	600m	YBCO	1 phase 1 cryostat	138 kV, 2.4kA	77 K	[MAGU11]
Yokohama, Sumitomo	2013	250 m	BSCCO	3 phase 1 cryostat	66 kV, 1.75 kA	69 – 73 K	[HIRO13]
Essen, Nexans	2014	1000 m	BSCCO	3 phase concentric	10 kV, 2.3 kA	67 K	[AMPA13]
Jeju Island, KEPCO	2015	1000 m	?	1 phase 1 cryostat	154 kV, 3.75 kA	72 K	[GEON20]

It can be clearly seen in the Table 2.2 that progress is being made throughout the years: the first superconducting cables commissioned had shorter lengths and lower nominal current and voltage, and with the years, an increase in both nominal operating points and length can be appreciated.

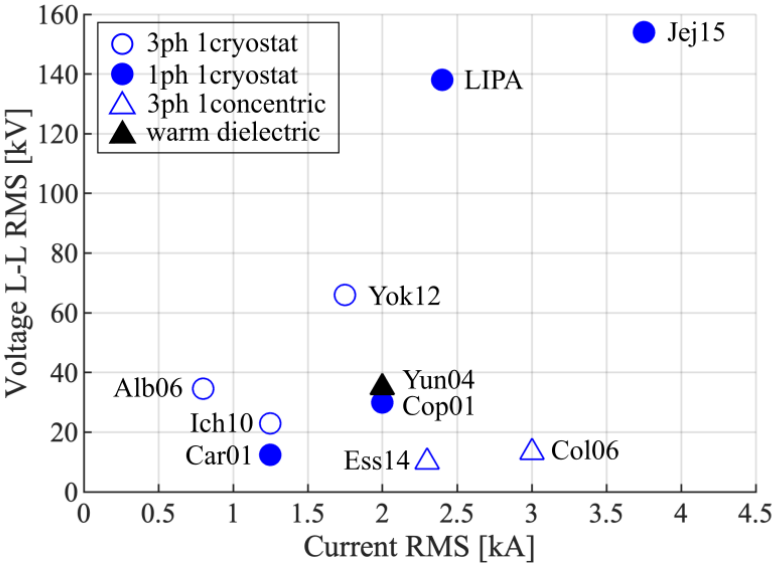

Figure 2. 5: IV map of commissioned AC HTS cables

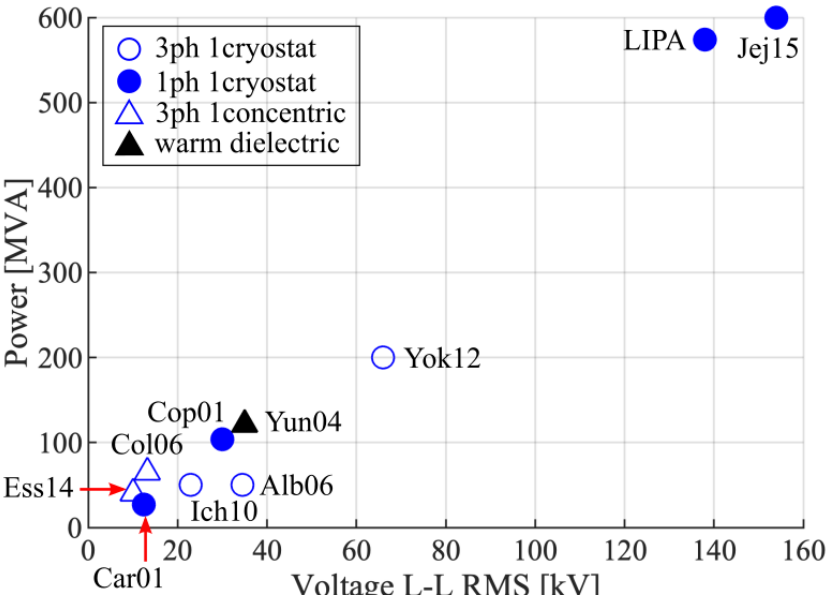

Figure 2. 6: PV map of commissioned AC HTS cables

Figures 2.5 and 2.6 provide a graphic representation of Table 2.2. These representations outline the fact that cables sharing the same architecture have similar nominal voltage and current. For example, in 2.6 the cables with 3 phase concentric configuration is used for the lowest nominal voltage applications while only the 1 phase 1 cryostat configuration is used when the nominal voltage exceeds 100 kV.

CHAPTER 3 – PROJECT DEFINITION

3.1 PROJECT OBJECTIVES

As it can be seen in the state of the art, several HTS cables have been already commissioned. But each of them has been conceived independently, using a different model, hence the lack of standardization. The main objective of this project is to contribute to the standardization of superconducting cables. To do so, we propose a framework for the multiphysics design of superconducting AC cable. The goal is to speed up the design phase of a superconducting cable by creating a model that characterizes any HTS cable system.
In addition, experimental work is carried out in the laboratory for the construction of a superconducting cable core testing facility that will allow to characterize cables. The objective is to create a test bench consisting of a cryostat, terminals, and the measuring device necessary to be able to automatize the extraction of the IV characteristic of superconducting cable core.

3.2 ORIGINALITIES

The framework for the design of the cable system is largely inspired from the work of D. Kottonau [KOTT19], but some modifications, improvements and corrections have been made to each model and to the framework. Beside, all the models are now implemented in Matlab so that they can be called from a single routine. This allows us to easily carry out additional analyses that complete [NOE_17].

The experimental work reported here is fully original. This includes the construction of the testbench (Chapter 7), the protocol for welding the superconducting cable core to its connector, and the protocol for the measurement of the superconducting tape I-V curve following the standard [ISN_03].

3.3 SYSTEM OVERVIEW

A superconducting cable system is formed by three main components:

- Cable core,
- Line Cryostat
- Terminals.

3.3.1 ASSUMPTIONS

Out of all the possible configurations seen on the state of the art, we restrict ourselves to the 1 phase 1 cryostat configuration. We consider HTS materials. The coolant is liquid nitrogen, it will only flow inside the former, without return path.

3.3.2 CABLE CORE

The cable core is made of several layers. From the inner part of the cable to the outer part, one will find the following layers: former, HTS conductor, dielectric insulation, HTS shield and neutral conductor.

3.3.2.1 Former

The former, also called inner tube, is a hollow tube which serves two functions: it acts as the mechanical support for the other layers and allows the flow of liquid nitrogen inside the tube. In the case of a short circuit, it may also carry part of the short circuit current [KOTT19].

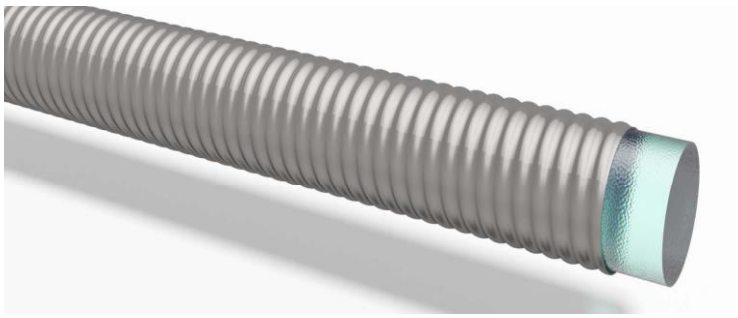

Figure 3. 1: Spiral corrugated tube former [4]

In the scope of this study, two types of formers will be treated: the Hollow Conductor (HC) former and the Corrugated Tube (CT) former. More details on each of these options will be provided in the design model.

3.3.2.2 HTS conductor layer

The HTS conductor layer is composed of several sub-layers of superconducting conductors. The conductors are mainly in form of tapes, either bismuth strontium calcium copper oxide (BSCCO) or yttrium barium copper oxide (YBCO). Each sub-layer is composed of several parallel HTS tapes of 2 to 12 mm of width arranged on the surface of the former. Its function is to provide a path for the current in normal operation.

Figure 3. 2: HTS Conductor layer [NOE_17]

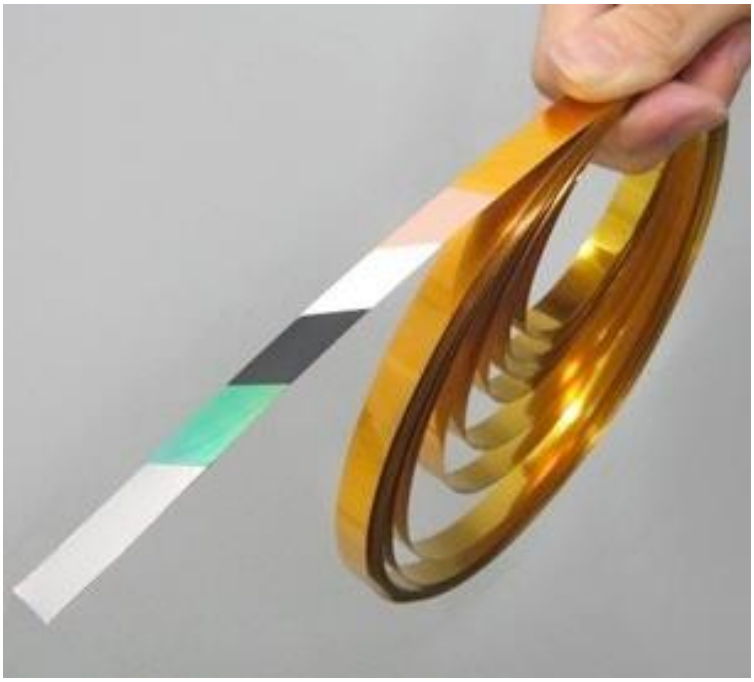

Figure 3. 3: HTS tape [TPIN19]]

3.3.2.3 Electrical Insulation layer

The electric insulation layer provides electrical insulation between the HTS conductor layer and the outer layers of the cable core. It is often made of Polypropylene Laminated Paper (PPLP) or High-Density Polypropylene (Tyvek) [KOTT19].

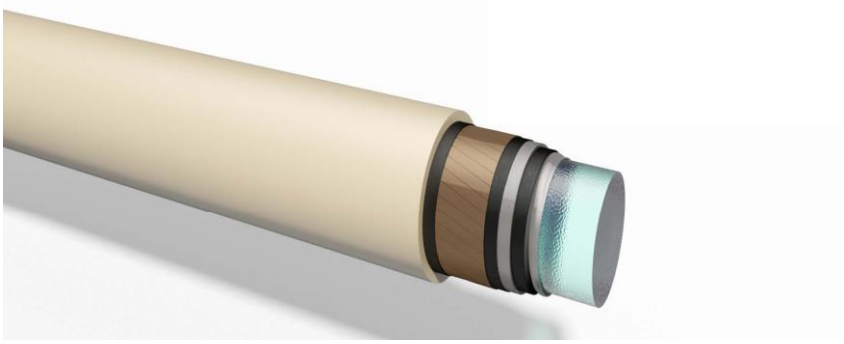

Figure 3. 4: Insulation layer [NOE_17]

3.3.2.4 HTS Shield layer

The HTS shield layer is made of a single layer of superconducting conductors. Its function is to shield the magnetic field of the cable. Each shield layer of each core is connected to each other at both ends of the cable, so that an electrical current of the same magnitude as the one flowing through the HTS conductor is induced in the HTS shield layer in the reverse direction, therefore reducing the electromagnetic field outside the cable to zero [MASU15].

3.3.2.5 Neutral Conductor layer

The neutral conductor layer is made of one or several layers of copper tapes. It is used both for structural support and as a pathway for fault currents.

3.3.2 LINE CRYOSTAT

The line cryostat maintains the temperature of the cable core at the target operation temperature. It is usually made of five layers: inner cryostat, superinsulation, vacuum, outer cryostat and mantel or jacket.

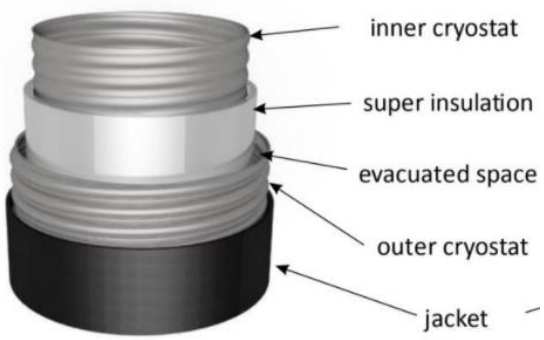

Figure 3. 5: Parts of the line cryostat [KOTT19]

In this study, the inner and outer cryostats are assumed to be made of a corrugated tube (CT). The super-insulation is wrapped on the outside on the inner cryostat tube and consists of ten to 30 layers of polyester foil vaporized with aluminum [KOTT19]. The mantel is made of Polyethylene (PE).

3.3.3 TERMINALS

The terminals are the components located at both ends of the cable which enable the transfer of current from the HTS cable system to the grid. Its function is to maintain the cable at its target operation temperature while transferring the current from the cable core to the grid using a current lead. It often connects to the liquid nitrogen pumping system as well.

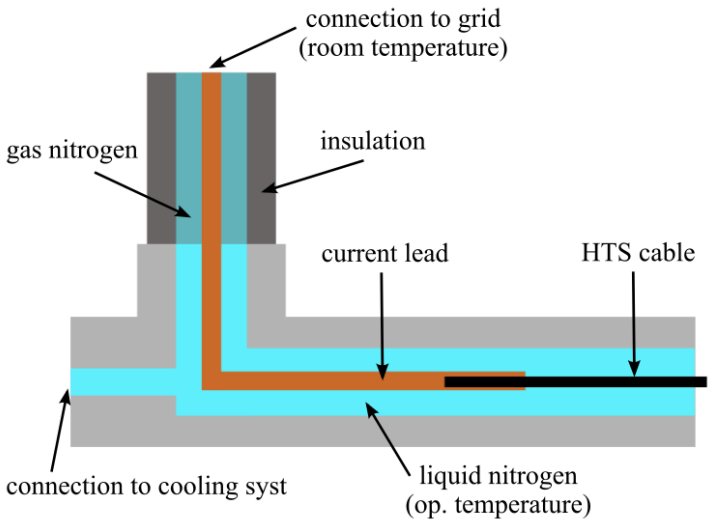

Figure 3. 6: HTS Cable terminal.

3.4 OPERATION RANGE

The choice of the operation range of a superconducting cable relies on mechanical, hydraulic, electrical, and thermal considerations.

According to the manufacturer [CRYO12], the maximum permissible pressure on the former and inner cryostat is 20 bar. Thus, for this study, the maximal operation pressure is fixed at 15 bar.

The nitrogen must remain liquid so that it can flow in the line cryostat and cool down the cable core. Any solidification could disrupt the flow of liquid nitrogen. The solidification temperature of nitrogen is 63.23 K thus, to avoid any solidification, the minimal operation temperature of the nitrogen is fixed at 68 K.

The formation of nitrogen gas must also be avoided to avoid possible electrical breakdown. To comply with this limitation, the maximal operation temperature of the nitrogen is set at 78 K and the minimal operation pressure of the liquid nitrogen is set to 3 bar, assuring sufficient safety margin to the nitrogen boiling line.

As a result, the operation range is limited by the blue area on Figure 3.7, where the chosen operation range is far from the orange evaporation line of liquid nitrogen.

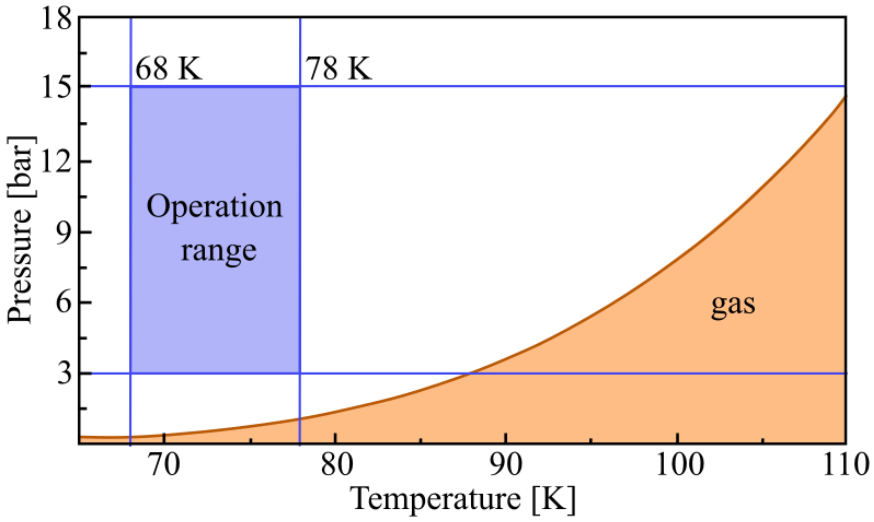

Figure 3. 7: Operation range of the superconducting cable system

CHAPTER 4 – DESIGN FRAMEWORK

In the scope of this project, a numerical model that characterizes a superconducting cable will be designed and implemented. The model will be able to recreate the internal geometry of the cable, specifying the thickness and material of each layer; it will create a hydraulic profile of liquid nitrogen inside the cable to verify pressure levels; a temperature profile of every point in the cable system, and it will also provide the user with all the thermal and electrical losses that the system would entail.

4.1 OVERVIEW

In this chapter, a framework to design superconducting AC cables is proposed and described. The proposed methodology has been adapted from the one proposed on [NOE_17].

Figure 4.1 illustrates the methodology for the cable design code, where one starts by stating the specifications of the cable as well as the physical parameters related to the superconducting tapes that are to be used.

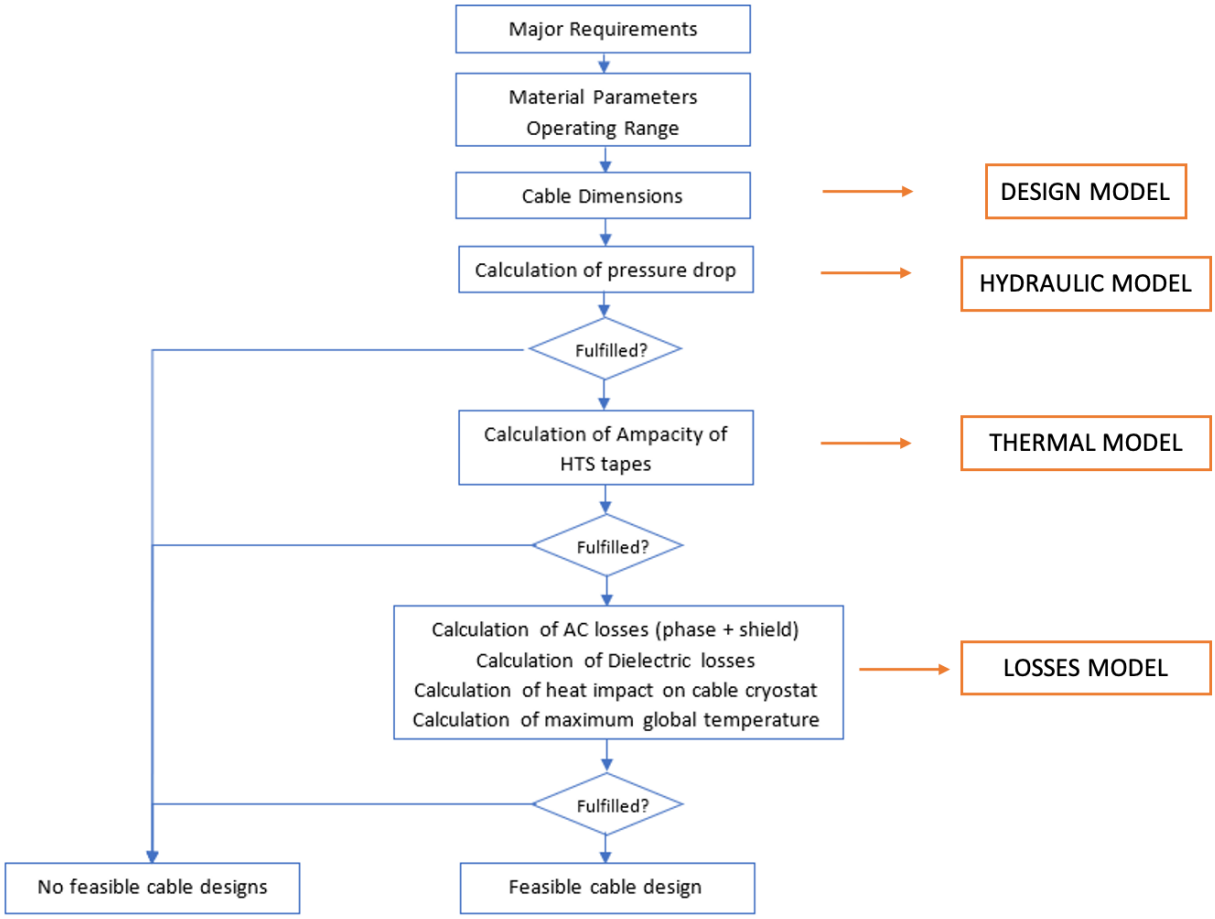

Figure 4. 1: Proposed methodology for cable design

The design framework is made of four models: cable layout model, hydraulic model, thermal model, and losses model.

The first step is the layout model, in charge of defining the dimensions of the various layers of the cable core and the line cryostat.

Next is the hydraulic model. The input of the model is the cable layout, and its output is the pressure at the cable's outlet. With the pressure at outlet, the routine verifies if the pressure drop is within the allowed operation range. Once the pressure distribution has been obtained, a pressure check is performed by the routine. If satisfactory, the design can continue.

Next is the thermal model. To keep its superconducting properties, the cable system must be in the temperature range. The thermal model estimates the distribution of the temperature both axially and radially. This model allows to monitor if at any point in the cable the maximum or minimum operating temperature boundaries are exceeded, and thus to know if the proposed cable design is feasible or not. Moreover, it also provides the temperature profile in the HTS

conductor and HTS shield layers, which are essential for calculating the total AC losses of the cable system. Once the temperature distribution has been obtained, a temperature check is performed by the routine. If satisfactory, the design can continue.

Next is the losses model. Although superconducting cables don't involve Joule losses, the heating of the nitrogen is produced, on one hand, by the electrical losses (dielectric losses and AC losses) of the cable inside the cryostat, and, on the other hand, by the heat input coming from outside of the cable system. These losses cannot be neglected if a technical feasibility study must be made. The calculation of each loss will be performed by this model.

The different models will have to be coupled with each other according to Figure 4.2.

In the following chapters, the various models are described in their order of appearance in the methodology: layout, hydraulic, thermal and losses model.

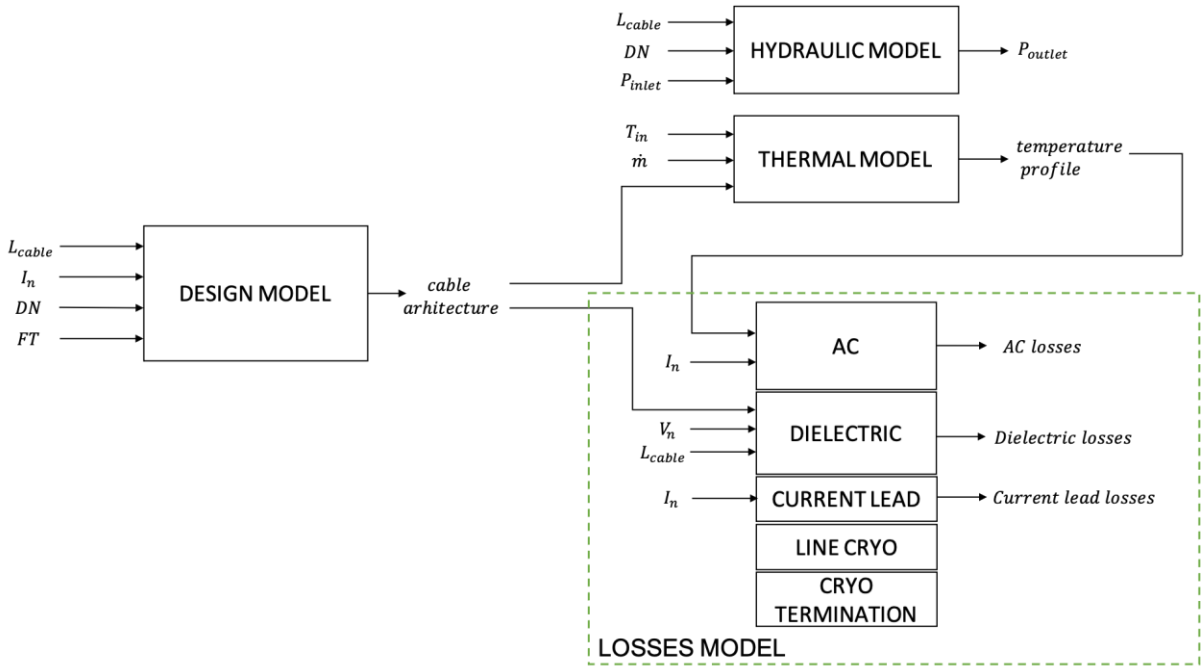

Figure 4. 2: Block diagram of functions for the cable design

4.2 LAYOUT MODEL

The goal of the layout model is to obtain the cable architecture. The idea behind this model is to build each layer starting from the inner layer ie. the former.

The inputs are the length of the cable L_{cable}, the nominal RMS current I_n, the former type *FT*, and the reference of the former *DN*. The output is a table describing the cable architecture.

The model is largely inspired from [KOTT19]. It is further developed here to allow for systematic design and implementation in the Matlab routine.

4.2.1 ASSUMPTIONS

We consider the one phase one cryostat configuration with cold dielectric.

Figure 4. 3: Block diagram of hydraulic model

We consider two different former types (FT): Hollow Conductor (HC) former and Corrugated Tube (CT) former. Table 4.1 summarizes the model.

Table 4. 1: Overview of design model

Symbol	Description	Unit
Inputs		
I_r	Rated L-N nominal current of cable system	A
L_{cable}	Total length of cable core	m
FT	Former type	-
DN	Inner former diameter	mm
Parameters		
α_{drill}	Twist angle of HTS tape	°
k_{SI}	Load factor	-
w_{tape}	HTS tape width	m
I_c	Critical current of HTS tape	A

Outputs		
cable_architecture	Cable architecture	-
HTS_cond_length	HTS material quantity	m

4.2.2 CABLE CORE

4.2.2.1 Former

Hollow Conductor

The Hollow Conductor concept is modelled after the conventional oil pressure cable. The Hollow Conductor concept will be modelled after a 138 kV, DN 20 oil internal pressure cable installed by Edison-Sault Electric Co. in 1975, [BURN18]. This type of cable, as it is outlined in [KOTT19], requires an additional copper layer made of copper wires, adding up an additional 300 mm^2 of cross-sectional area to the former on top of the 2 mm thickness of the hollow pipe. Figure 4.4 shows the cross-sectional area of the referenced oil cable next to a scale, which allows us to confirm the additional 300 mm^2 taken up by the copper wires and thus, to validate this information so it can be used in the cable design procedure.

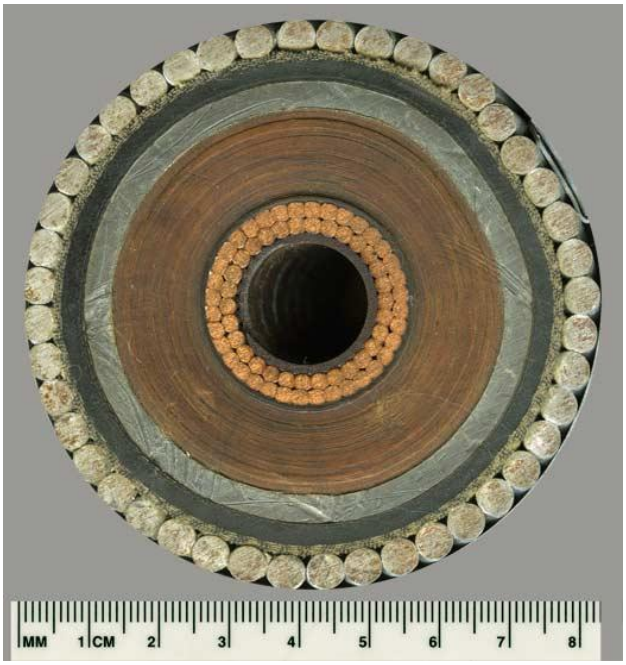

Figure 4. 4: 138 kV Edison-Sault Electric Co. submarine cable [BURN18]

Taking the inner diameter of the former as a variable and using the 300 mm^2 hypothesis, the outer diameter of the former can be obtained using (1) and (2).

$$D_{i,Cu} = D_{i,former} + 0.002 \quad (1)$$

$$S_{Cu} = \pi\left(\frac{D_{o,former}^2}{4} - \frac{D_{i,Cu}^2}{4}\right) \quad (2)$$

S_{Cu}	Additional copper layer surface	[m^2]
$D_{i,Cu}$	Inner diameter of additional copper layer	[m]
$D_{o,former}$	Former outer diameter	[m]
$D_{i,former}$	Former inner diameter	[m]

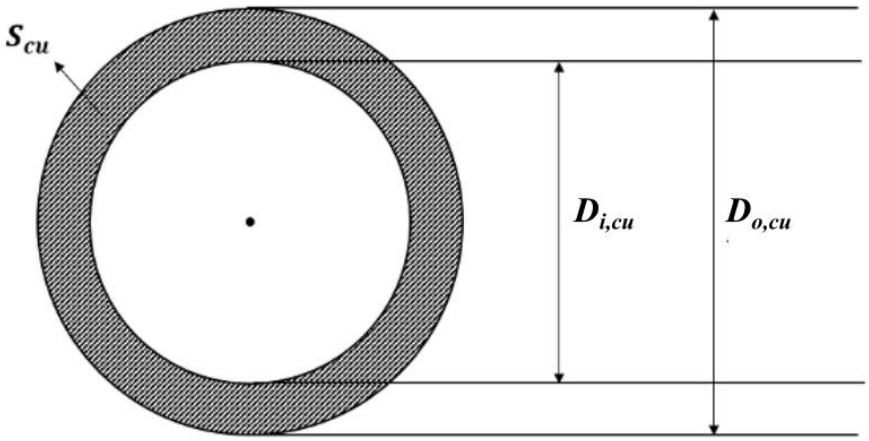

Figure 4. 5: Hollow Conductor 2D schema

Corrugated Tube

The Corrugated Tube former is modeled after the standard for corrugated metal hoses [ISO_12]. Thus, for the three inner former diamters evaluated in this study, the former outer diameter can be directly extracted from Table 4.2.

Table 4. 2: Former diameters for the evaluated DN

Reference of the former	Inner former diameter [mm]	Outer former diameter [mm]
DN 32	32	34.2
DN 40	40	42.8
DN 50	50	52.8

4.2.2.2 HTS Conductor Layer

Number of HTS tapes

This layer is made up of one or several layers of superconducting tapes wound one next to the other. The number of tapes needed to fulfil the specifications of a cable are established by both electrical and geometrical constraints.

To construct the HTS conductor layer, the model starts by determining how many superconducting tapes are required to fulfill the nominal current specification [KOTT19]:

$$N_{tapes,elec} = \frac{\sqrt{2} \cdot I_r}{k_{SI} \cdot I_c} \quad (3)$$

$N_{tapes,elec}$	Electrically required number of tapes	[-]
I_r	Rated RMS current	[A]
k_{SI}	Load factor	[-]
I_c	Critical current of a tape conductor	[A]

The load factor k_{SI} is the percentage of the critical current I_c that can flow in each tape.

Equation (3) gives the minimal number of tapes that the cable must have in order to carry the nominal current, but how the tapes will be distributed into layers is decided by geometrical constraints. To calculate the number of tapes that can be laid one next to another on the same layer, the outer diameter of the former is taken as the diameter of the largest circle that can be inscribed in a polygon of n_i sides of side length equal to the w_α (Figure 4.6). w_α is the effective tape width after twisting of the tape on the former with a twist angle α.

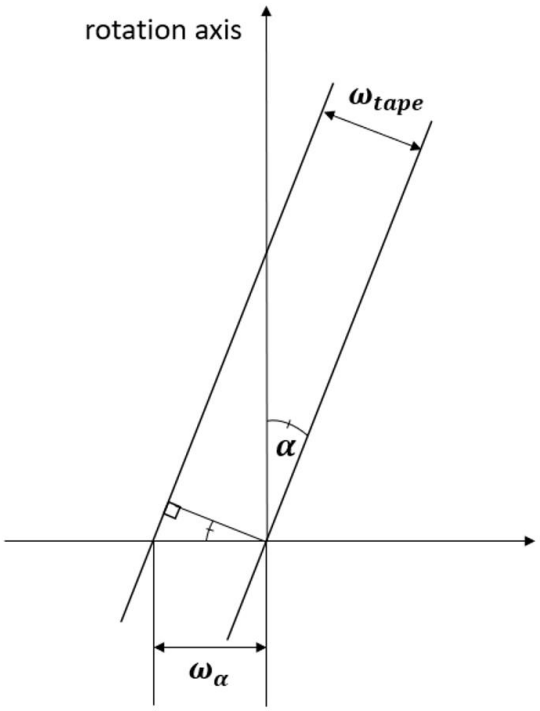

Figure 4. 6: Schematic explanation of width w_α

$$w_\alpha = \frac{w_{tape}}{\cos\left(\alpha_{drill}\right)} \qquad (4)$$

[MATH21] was used to obtain equations (5) and (6) and thus to obtain the number of geometrically required tapes.

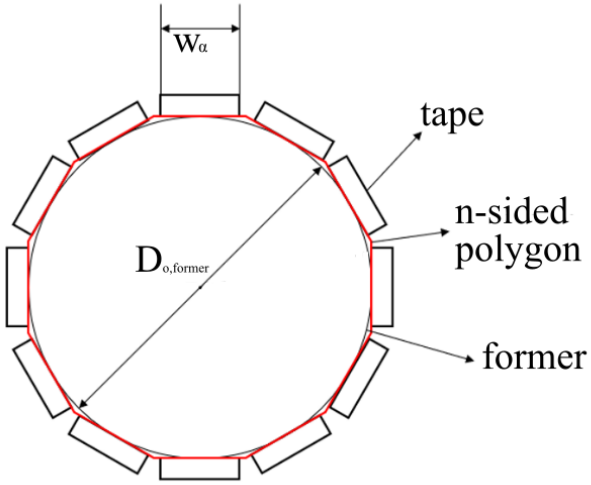

Figure 4. 7: Schematic representation of the circumference inscribed in a polygon of n_i sides.

$$D \cdot \tan\left(\frac{\pi}{n_i}\right) > w_\alpha \qquad (5)$$

$$n_i < \frac{\pi}{\operatorname{atan}\left(\frac{w_\alpha}{D}\right)} \qquad (6)$$

$$n_i = floor\left(\frac{\pi}{\operatorname{atan}\left(\frac{w_\alpha}{D}\right)}\right) \qquad (7)$$

α_{drill}	Twist angle	[°]
w_α	Cross-sectional tape width	[m]
w_{tape}	HTS tape width	[m]
D	Outer diameter for layer i	[m]
n_i	Number of geometric tapes on layer i	[-]

Equations (4) to (7) allow to determine how many tapes can fit geometrically one next to another for a given former. Depending on the diameter, one or more layers will need to be applied. The key to is to add on layers until the total number of geometrical tapes is equal or larger than the electrically required number of tapes, while bearing in mind that once a layer is added, it must be complete. Every time a layer is added, its thickness must be considered to recalculate the inner diameter for the new layer.

$$N_{tapes} = N_{tapes,geo} \geq N_{tapes,elec} \quad (8)$$

Total length of HTS conductor

For economic considerations it is necessary to know how much superconducting material is being used in the cable system. To do so, one must know the tape length L_{tape} which, since the tape is twisted along the length of the cable, is greater than the length of the cable [KOTT19],

$$L_{tape} = \frac{L_{cable}}{\cos(\alpha)} \quad (9)$$

Knowing the tape length and the total geometric number of HTS tapes used to construct the cable system, the total length of HTS tape can be calculated.

$$L_{HTScond} = \sum_{i=1}^{n_{layers,geo}} n_i \cdot l_{drill} \quad (10)$$

L_{tape}	Total tape length	[m]
L_{cable}	Total cable length	[m]
$L_{HTScond}$	Total HTS tape length for cable system	[m]
$n_{layers,geo}$	Number of layers of HTS tape	[-]
n_i	Number of HTS tapes in layer i	[-]

4.2.2.3 Electrical Insulation Layer

For the scope of this model, only high-density polyethylene (Tyvek) will be considered for the insulation. For this section, the results from [KOTT19] have been directly extrapolated, obtaining the following insulation thicknesses for the treated former dimensions:

Table 4. 3: Insulation thicknesses for Hollow Conductor former

Inner former diameter [mm]	Insulation thickness [mm]
DN 32	25.85
DN 40	24.15
DN 50	24.25

Table 4. 4: Insulation thicknesses for Corrugated Tube former

Inner former diameter [mm]	Insulation thickness [mm]
DN 32	25.85
DN 40	25.5

DN 50	24.0

4.2.2.4 HTS Shield Layer

The number of tapes needed for the shield is the number of tapes necessary to cover the whole surface of the insulation layer outer diameter with tapes. To calculate the required number of shield tapes is as simple as using equation (11) for the pertinent diameter.

$$N_{tapes,shield} = floor\left(\frac{\pi}{\text{atan}\left(\frac{w_\alpha}{D_{o,insulation}}\right)}\right) \quad (11)$$

The thickness of the shield layer is equal to the thickness of a shield tape, since just one layer of tapes is used to build it. The total length of tape required for the HTS shield layer is obtained with equations (9) and (10).

4.2.2.5 Neutral Conductor Layer

This layer consists of 2 mm copper tapes covering the surface of the outer HTS shield diameter. Thus, the thickness of the layer is of 2 mm.

4.2.3 LINE CRYOSTAT

4.2.3.1 Inner Cryostat

The inner cryostat is assumed to be a corrugated tube and thus its dimensions are obtained from follow the standard [ISO_12].

Table 4. 5: Inner cryostat dimensions [ISO_12]

CT reference	Inner cryostat ID [mm]	Inner Cryostat OD [mm]
DN 20	20	22.0
DN 25	25	27.2
DN 32	32	34.2
DN 40	40	42.8
DN 50	50	52.8
DN 65	65	68.4
DN 80	80	84.0
DN 100	100	104.6
DN 125	125	130.2
DN 150	150	156.2

4.2.3.2 Outer Cryostat

The design of the outer cryostat must follow the constraint that the inner and outer cryostat must be at least 10 mm apart. Using the standard [ISO_12], the idea is to find a DN from Table 4.5 that is at least 10 mm greater than the inner cryostat outer diameter and use it as inner diameter for the outer cryostat.

For the mantel, as seen in Figure 4.4, in conventional underground cables, the cable is surrounded by a 5 mm thick, protective Polyethylene (PE) [KOTT19].

4.3 HYDRAULIC MODEL

The objective of the hydraulic model is to calculate the pressure drop due to hydrostatic and hydrodynamic losses and verify that at the outlet the pressure of the liquid nitrogen is still within the fixed operational range.

Figure 4. 8: Block diagram of hydraulic model

This model is the model presented in [KOTT19] but some corrections have been made to it (see equation (14)). It takes as an entry the diameter of the cavity where the liquid nitrogen will flow, also called the former, as well as cable length and height difference between inlet and outlet and provides the total pressure loss of the system. Pressure drop inside the former can be due both to hydrostatic and hydrodynamic pressure losses.

Both former types will be modelled after a smooth pipe for the flow of liquid nitrogen. Table 4.6 summarizes the hydraulic model.

Table 4. 6: Recapitulative of hydraulic model

Symbol	Description	Unit
Inputs		
P_{inlet}	Pressure at cable inlet	Pa
L_{cable}	Total length of cable core	m
$\dot{m}$	LN2 mass flow	kg/s
DN	Inner former diameter	mm
Parameters		
$P_{op,max}$	Maximum operation pressure	Pa
$P_{op,min}$	Minimum operation pressure	Pa
Outputs		
P_{outlet}	Pressure at cable outlet	Pa

4.3.1 ASSUMPTIONS

There is no specific assumption.

4.3.2 HYDRODYNAMIC PRESSURE LOSS

There is no specific approach in the literature on how to obtain the hydrodynamic pressure loss for the two architectures that are treated in this study: Corrugated Tube pipe and Hollow Conductor pipe. So, for the scope of this study, the Bernoulli-formed Darcy-Welsbach equation for a flat smooth pipe (equation (15)) will be used. To be able to solve this equation, it is necessary to obtain first the pipe friction coefficient λ_R, obtained implicitly through equation (12)

$$v_F = \frac{\dot{m}}{\rho_{LN}\, A_{IF}} = \frac{\dot{m}}{\rho_{LN}\left(\frac{\pi d_{IF}^2}{4}\right)} \qquad (12)$$

$$Re_{IF} = \frac{v_{IF}\, d_{IF}\, \rho_{LN}}{\eta_{LN}} \qquad (13)$$

$$\frac{1}{\sqrt{\lambda_R}} = 2log\left(\frac{Re_F\sqrt{\lambda_R}}{2.51}\right) \qquad (14)$$

$$\Delta p_{HD} = \frac{\lambda_R\, L_{cable}}{d_{IF}} \cdot \frac{\rho_{LN}}{2} \cdot v_{IF}^2 \qquad (15)$$

Δp_{HD}	Hydrodynamic pressure loss inside former	[Pa]
Re_{IF}	Reynold's number inside former	[-]
λ_R	Pipe friction coefficient	[-]
L_{cable}	Length of cable	[m]
d_{IF}	Inner diameter of former	[m]
ρ_{LN}	Density of liquid nitrogen	[kg/m³]
η_{LN}	Dynamic viscosity of liquid nitrogen	[kg/m·s]
v_{IT}	Flow rate of the liquid inside the former	[m/s]
$\dot{m}$	Mass flow	[kg/s]

The key factors affecting hydrodynamic pressure loss are both the inner diameter of the former and the mass flow of liquid nitrogen as they have an impact of order five and two respectively on the pressure loss result.

4.3.3 HYDROSTATIC PRESSURE LOSS

If the cable were not to lay fully horizontal ($\Delta h \neq 0$), the difference in height between inlet and outlet results in an additional loss of pressure. Equation (16) accounts for the hydrostatic pressure loss:

$$\Delta p_{HS} = g \cdot \rho_{LN} \cdot \Delta h \qquad (16)$$

Δp_{HS}	Hydrostatic pressure loss inside former	[Pa]
g	Acceleration of gravity, 9.81 m/s^2	[m/s^2]
Δh	Height difference	[m]

Since both hydrostatic and hydrodynamic pressure loss can occur at the same time, it is necessary to take both into account for the pressure drop calculation, Δp, which yields:

$$\Delta p = \Delta p_{HS} + \Delta p_{HD} \qquad (17)$$

4.4 THERMAL MODEL

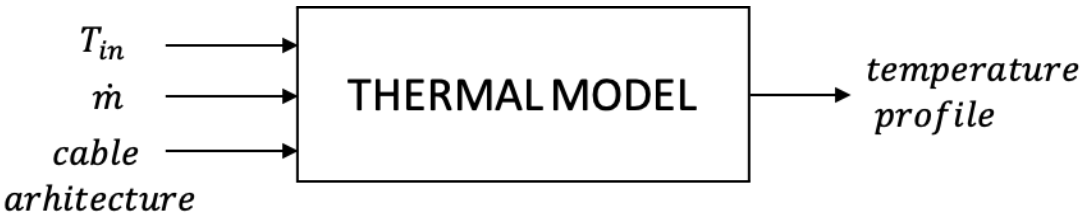

Figure 4. 9: Block diagram of thermal model

The role of the thermal model in the cable system design is to compute the temperature profile at all points of the cable system so that the design protocol can then check if the operational temperature boundaries are respected. The idea behind this model is a finite difference method calculation is based on the open-source code [SOUS20], which has been adapted to the architecture of the cable analyzed in this study.

To obtain the temperature profile at every point of the cable, the system is interpreted under cylindrical coordinates, and it is discretized along the length and the radius as shown in Figure 4.10.

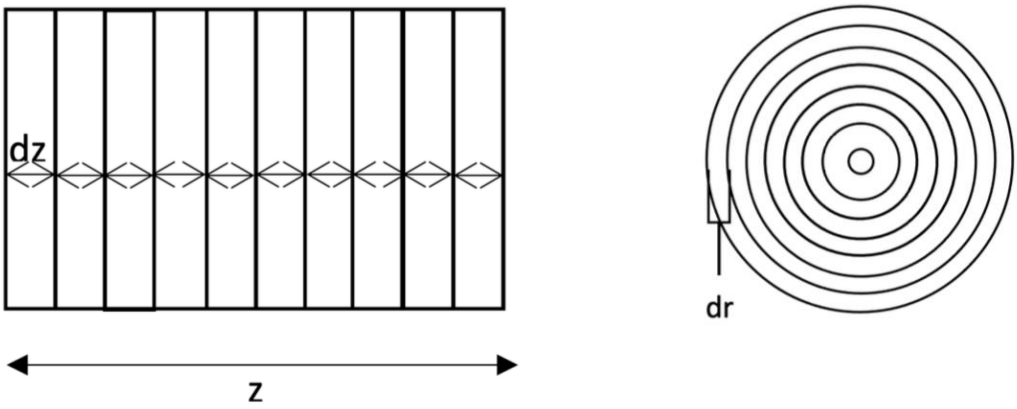

a) Axial Discretitation *b) Radial Discretization*

Figure 4. 10: Discretization of cable system for FDM method

The model works in such way that the temperature profile of the cable system can be calculated by just providing the temperature of the liquid nitrogen at the inlet, the liquid nitrogen flow and the concrete dimensions of the cable's layers and length.

Table 4. 7: Overview of the thermal model

Symbol	Description	Unit
Inputs		
T_{in}	Temperature of LN2 at cable inlet	K

L_{cable}	Total length of cable core	m
$\dot{m}$	LN2 mass flow	kg/s
cable_architecture	Cable architecture	-
Parameters		
w_{tape}	Tape width	m
Outputs		
T	Temperature profile of cable	K

4.5 LOSSES MODEL

For this model, the assumption made on each type of loss are cited in their corresponding section. Figure 4.11 gives an overview of the model:

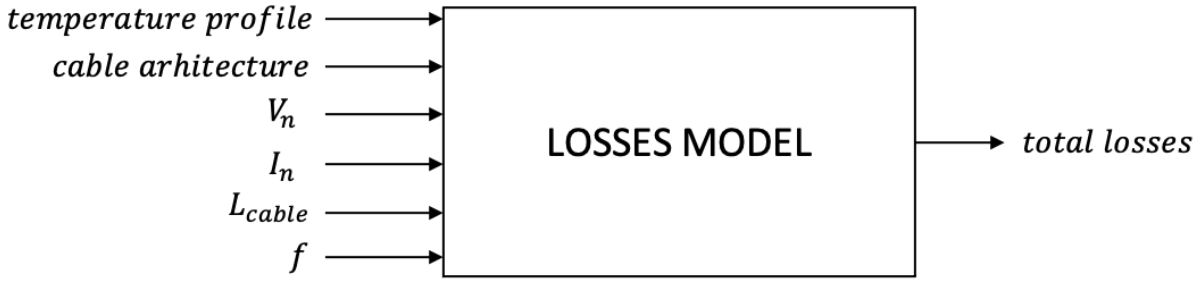

Figure 4. 11: Block diagram of Losses Model

4.5.1 ASSUMPTIONS

For the calculation of losses, the following assumptions are made:

4.5.2 AC LOSSES IN HTS AND SHIELD LAYERS

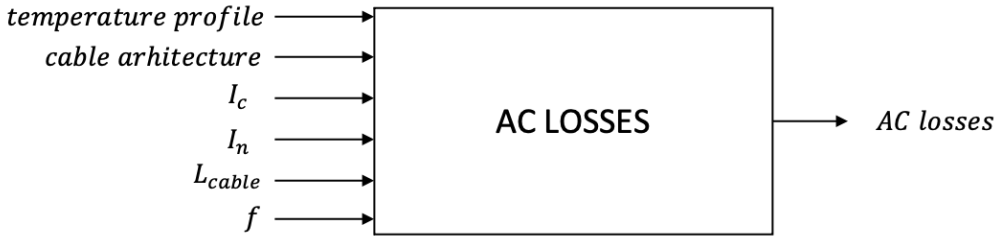

Figure 4. 12: Block diagram of AC losses

Table 4. 8: Overview of AC losses

Symbol	Description	Unit
Inputs		
T	Temperature profile of cable	K
I_r	Rated L-N nominal current of cable system	A
cable_architecture	Cable architecture	-
Parameters		
f	Network frequency	Hz
I_c	Critical current of HTS tapes	A
T_c	Critical temperature of HTS tapes	K

T_0	SF temperature of HTS tapes	K
Outputs		
AC_losses	Sum of AC losses of shield and HTS conductor for the whole cable system	W

The following equation system allows to obtain the AC losses separately for both the HTS conductor and the shield depending on the temperature profile in the layer.

$$\hat{I}_t = \frac{I_N\sqrt{2}}{n_{tapes}} \quad (18)$$

$$I_c(T) = I_{c0}\left(\frac{T_c - T}{T_c - T_0}\right) \quad (19)$$

$$P_{hyst} = \frac{\mu_0 \cdot f \cdot I_c^2(T)}{\pi}\left[\left(1 - \frac{\hat{I}_t}{I_c(T)}\right) log\left(1 - \frac{\hat{I}_t}{I_c(T)}\right) + \left(1 + \frac{\hat{I}_t}{I_c(T)}\right) log\left(1 + \frac{\hat{I}_t}{I_c(T)} - \left(\frac{\hat{I}_t}{I_c(T)}\right)^2\right)\right] \quad (20)$$

$$P_{AC/L}(T) = \sum_{i=1}^{n_{layers}} P_{hyst}(I,T) \cdot n_{l,t} \quad (21)$$

I_N	Nominal rated current of the cable	[A]
$\hat{I}_t$	Peak current	[A]
n_{tapes}	Number of HTS tapes	[-]
I_C	Critical current of HTS tape	[A]
$I_C(T)$	Critical band current	[A]
T_C	Critical temperature of HTS tape	[K]
T_0	Reference temperature	[K]
P_{hyst}	Tape hysteresis loss per unit length	[J/m]
μ_0	Magnetic field constant	[kgm/s^{2}A^2]
a	Exponent of temperature dependence	[-]
n_{layer}	Number of layers of HTS conductor	[-]
$n_{t,l}$	Number of tapes per layer	[-]
$P_{AC/L}$	Cable hysteresis losses per unit length	[W/m^2]

4.5.3 DIELECTRIC LOSSES

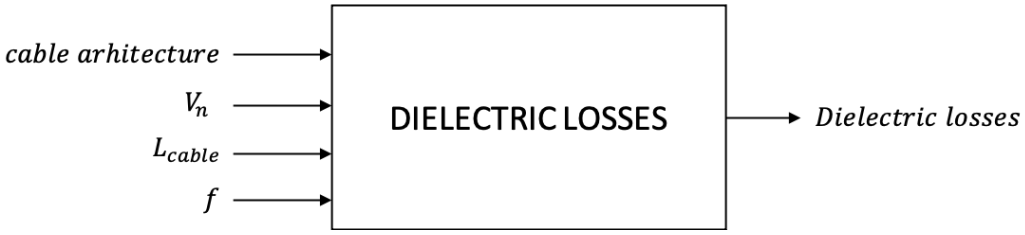

Figure 4. 13: Dielectric losses block

Table 4. 9: Overview of dielectric losses

Symbol	Description	Unit
Inputs		
L_{cable}	Total length of cable core	L
V_n	Rated L-N nominal voltage of cable system	V
cable_architecture	Cable architecture	-
Parameters		
f	Network frequency	Hz
$\boldsymbol{I_c}$	Critical current of HTS tapes	A
Outputs		
Dielectric_loss	Dielectric losses of cable system	W
C	Cable core capacitance	F

Dielectric losses are the result of the dissipation of energy due the movement of charges in an alternating electromagnetic field as polarization switches direction. Following [IEC_60], the dielectric losses are calculated using,

$$C = \frac{\varepsilon_{TY} \cdot 10^{-9}}{18 \cdot ln\left(\frac{r_{o,ins}}{r_{i,ins}}\right)} \quad (22)$$

$$P_{dielec} = 2\pi f \cdot C \cdot tan(\delta) \cdot U_{LE}^2 \quad (23)$$

P_{Dielec}	Dielectric losses of insulation	[W/m]
C	Capacity flooring	[F/m]
tan (δ)	Loss factor of isolation (1.3e-4)	[-]
ε_{TY}	Relative permittivity of Tyvek insulation=1.73	[F/m]
$r_{o,ins}$	Outer radius	[m]

$r_{i,ins}$	Inner radius	[m]
V	Cable rated voltage [L-N RMS]	[V]

4.5.4 LINE CRYOSTAT LOSSES

Line losses are mainly dependent on the quality of the thermal insulation.

The heat transfer takes three forms: radiation, convection, and conduction. We assume that both conduction and convection can be neglected [KOTT19].

The line cryostat losses are generally given by the cryostat manufacturers in the product's data sheet. Looking carefully at the two latest catalogues of Transfer lines for Liquid gases [CRYO12] and [CRYO15], one can choose the most loss reducing cryostat, being this Cryotherm's flexible deign cryostat which has a **1.3 W/m** line loss.

4.5.5 TERMINATION CURRENT LEAD LOSSES

Both thermal and electrical losses take place in the current lead. The electrical losses are created by the Joule effect (since the terminations are conventional conductors), and the thermal losses occur due to the heat transfer crated by the difference in temperatures between the environment and the cable system.

Table 4. 10: Overview of Termination current lead losses

Symbol	Description	Unit
Inputs		
I_r	Rated L-N nominal current of cable system	A
Outputs		
Current_lead_loss	Total current lead losses of system	W

According to the literature, [HERR93] the total amount of losses for one current lead at 77 K is of 0.45 W/A. In [KOTT17] it is stated that through experimental results, 37% of these losses are accounted as thermal losses, while the remainder 63% are electrical, Joule effect losses,

$$P_{CL} = P_{CL,th} + P_{CL,el} \quad (24)$$

$$P_{CL} = 0.045 \cdot I_r \cdot \left(0.37 + 0.63\left(\frac{I}{I_r}\right)^2\right) \quad (25)$$

P_{CL}	Current lead losses	[W]
$P_{CL,th}$	Thermal losses in current lead	[W]
$P_{CL,el}$	Electrical losses in current lead	[W]
I_r	Rated current of cable	[A]
I	Nominal current of cable	[A]

4.5.6 TERMINATION CRYOSTAT LOSSES

The termination cryostat losses are attributed to the heat transfer taking place through the walls of the termination. According to [KOTT19], they are load-independent and expected to be $\mathbf{P_{v,0,EK}=20W}$ for each extremity.

CHAPTER 5 – OBTAINED RESULTS

5.1 CASE STUDY

We consider the 1 phase in 1 cryostat cold dielectric configuration. We consider two former types: hollow conductor former and corrugated tube former. We consider that the former inner diameters have 3 possible sizes: 32 mm, 40 mm, and 50 mm. These inner former diameters were chosen because they are already treated in [KOTT19] and thus will serve as a reference to compare the results provided by the model to previous research to prove the functionality of the model.

Table 5. 1: Possible cable configurations studied in the work

Cable Configuration	Former Type	Former diameter [mm]
1 phase 1 cryostat	Hollow Conductor (HC)	DN 32
		DN 40
		DN 50
	Corrugated Tube (CT)	DN 32
		DN 40
		DN 50

The case study that will be used is the one proposed by D. Kottonau [KOTT19] and summarized in Table 5.2.

Table 5. 2: Cable specification [31]

Symbol	Description	Value	Unit
Inputs			
L_{cable}	Total length of cable core	3200	m
U_n	Nominal Voltage [L-L, RMS]	380	kV
I_r	Nominal current [L-N, RMS]	3600	A

$\dot{m}$	LN2 mass flow	0.9	kg/s
T_{in}	Temperature of LN2 at cable inlet	68	K
P_{in}	Pressure of LN2 at cable inlet	3	bar
Parameters			
f	Network frequency	50	Hz
α_{drill}	Twist angle of tape	15	°
w_{tape}	HTS tape width	0.004	m
k_{SI}	Load factor	0.8	-
I_c	Critical current of HTS tapes	150	A
T_c	Critical temperature of HTS tapes	90	K
T_0	SF temperature of HTS tapes	77	K

The system is composed of 2 cable cores with three separate 1 phase 1 cryostat HTS cables to form a three-phase cable system. A one-side cooling concept is adopted so that liquid nitrogen can flow through all three phases requiring only one cooling system.

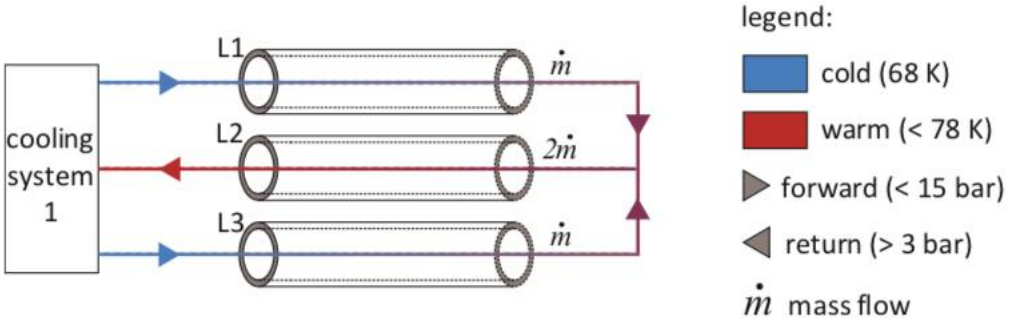

Figure 5. 1: One-side cooling concept [KOTT19]

Note that the liquid nitrogen needs to make its way back to the cooling system so it can be refrigerated again. This is achieved by the configuration shown in Figure 5.1, where "cold" nitrogen flows directly from the source to two of the phases and, when it has flowed through them, it becomes "warm" liquid nitrogen and makes its way back to the source by flowing through the third phase. As a result, the mass flow is doubled in the return path. It will also be this phase that will be most in danger of surpassing the operational temperature limits, as warmer liquid nitrogen will have less cooling potential.

The one-sided cooling configuration must be accounted for in the coupling of the hydraulic, thermal and losses model since the nitrogen will be undertaking a route of double length to the one selected in the cable specification.

In the next section, the results provided by the program for all six possible configurations will be analyzed.

5.2 HOLLOW CONDUCTOR (HC) RESULTS

5.2.1 HC DN 32

The configuration of a cable system of 32 mm of inner former hollow conductor diameter under one-sided cooling concept is not a feasible system because the pressure drop exceeds the minimum operational pressure that has been fixed in the "warm", returning nitrogen phase. Since this configuration is not possible in the hydraulic dimension, it is not feasible and thus cannot be analyzed because the design stops right after the pressure check. This design could become feasible if a two-side cooling concept was used, where "cold" nitrogen flows through all three phases.

5.2.2 HC DN 40

The configuration of a cable system of 40 mm of inner former hollow conductor diameter under one-sided cooling concept is not a feasible system because the pressure drop exceeds the minimum operational pressure that has been fixed in the "warm", returning nitrogen phase. Since this configuration is not possible in the hydraulic dimension, it is not feasible and thus cannot be analyzed. The same conclusion as in DN 32 is reached.

5.2.3 HC DN 50

The results obtained for a cable system of 50 mm of inner diameter of hollow conductor former under one-side cooling configuration are the following:

5.2.3.1 Cable Geometry

Table 5.3 and Figure 5.2 give an overall definition of the obtained cable geometry.

Table 5. 3: DN 50 HC cable's Geometry

	Layer	Thickness [m]	Outer Diameter [m]	Outer Radius [m]
1	LN2 IN	0.025	0.0500	0.0250
2	Former	0.037	0.0574	0.0287
3	Hollow Conductor	0.0002	0.0578	0.0289
4	HTS Conductor	0.0243	0.1063	0.0532

5	Insulation	0.0002	0.1067	0.0534
6	HTS Shield	0.0020	0.1107	0.0554
7	Neutral Conductor	0.0071	0.1250	0.0625
8	LN2 OUT	0.0026	0.1320	0.0651
9	Inner Cryostat	0.0099	0.1500	0.0750
10	Outer Cryostat	0.0030	0.1560	0.0780
11	Mantel	0.0050	0.1660	0.0830

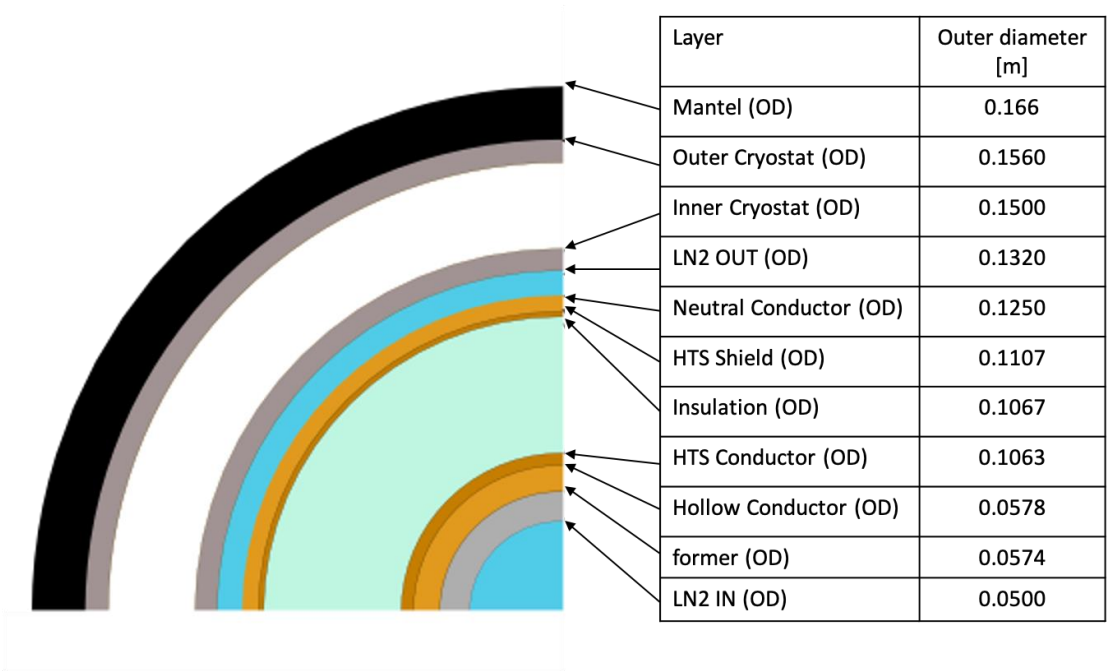

Figure 5. 2: Summary of cable geometry for DN 50 Hollow Conductor

Moreover, the design model provides the repartition of tapes in the HTS conductor and Shield layer, represented in Table 5.4, where the length of tape material is given for single phase.

Table 5. 4: DN 50 HC cable's HTS tape repartition per core

HTS layer	Tape layer	Number of tapes in layer	Layer thickness [m]	Total tape length [km]	Tape length per km [m]
HTS Conductor	Layer 1	43	0.002	142.45	44.53
HTS Shield	Layer 1	80	0.002	265.03	82.82

5.2.3.2 Hydraulic Results

This configuration complies with the set operational temperature range that sits between 3 bar and 15 bar.

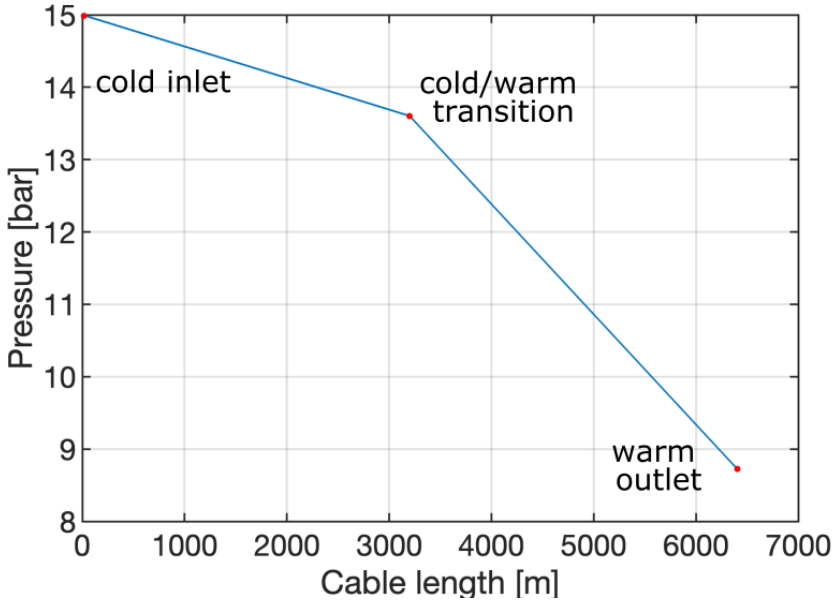

Figure 5. 3: DN 50 Pressure profile

Table 5. 5: DN 50 HC cable's key pressure points

Pressure at inlet of "cold" nitrogen [bar]	Pressure at warm/cold transition [bar]	Pressure at outlet of "warm" nitrogen [bar]
15.000	13.604	8.729

5.2.3.3 Thermal Results

The configuration respects the set thermal operational range for liquid nitrogen. Figure 5.4 displays the temperature of the liquid nitrogen flowing inside the former.

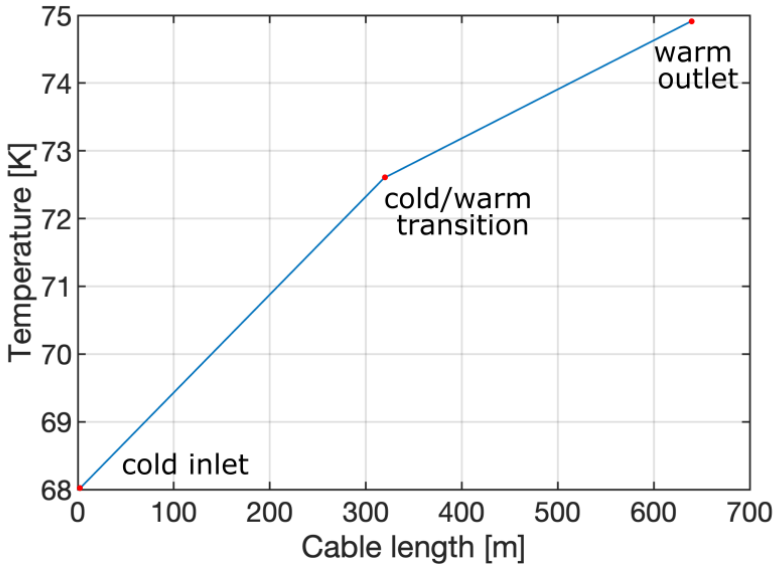

Figure 5. 4: HC DN 50 cable's Liquid nitrogen thermal profile

Table 5. 6: DN 50 HC cable's key thermal points

Layer	Temperature at "cold" inlet [K]	Temperature at cold outlet [K]	Temperature at "warm" inlet [K]	Temperature at "warm" outlet [K]
Liquid Nitrogen	68.00	72.61	72.61	74.92
HTS Conductor	68.02	68.58	72.63	72.91
HTS Shield	68.84	69.40	73.44	73.73
Cable's Maximum Global Temperature			**75.75 K**	

As it can be seen in the Figure 5.4 and Table 5.6, the temperature of the liquid nitrogen is within the operation range. Moreover, the maximum global temperature of the cable is also under the set operational temperature range.

5.2.3.4 Losses

Table 5.7 contains the estimated losses for the cable system.

Table 5. 7: Cable system losses for the DN 50 HC former

AC losses	10.022 kW
Current Lead losses	1.944 kW
Dielectric losses	5.995 kW
Line Cryostat losses	29.960 kW
Termination Cryostat losses	0.240 kW
Total System Losses	**43.161 kW**

5.3 CORRUGATED TUBE (HC) RESULTS

5.3.1 CT DN 32

The configuration CT DN32 (32 mm of inner former corrugated tube diameter) under one-sided cooling concept is not a feasible system because the pressure drop exceeds the minimum operational pressure that has been fixed in the "warm", returning nitrogen phase. Since this configuration is not possible in the hydraulic dimension, it is not feasible and thus cannot be analyzed because the design stops right after the pressure check. This design could become feasible if a two-side cooling concept was used, where "cold" nitrogen flows through all three phases.

5.3.2 CT DN 40

The configuration CT DN40 (40 mm of inner former corrugated tube diameter) under one-sided cooling concept is not a feasible system because the pressure drop exceeds the minimum operational pressure that has been fixed in the "warm", returning nitrogen phase. Since this configuration is not possible in the hydraulic dimension, it is not feasible and thus cannot be analyzed. The same conclusion as in DN 32 is reached.

5.3.3 CT DN 50

The results obtained for a cable system of 50 mm of inner diameter of corrugated tube former under one-side cooling configuration are the following:

5.3.3.1 Cable Geometry

Table 5.8 and Figure 5.5 give an overall definition of the obtained cable geometry.

Table 5. 8: CT DN50 cable's Geometry

	Layer	Thickness [m]	Outer Diameter [m]	Outer Radius [m]
1	LN2 IN	0.0250	0.0500	0.0250
2	Former	0.0014	0.0528	0.0264
3	Hollow Conductor	0.0004	0.0536	0.0268
4	HTS Conductor	0.0240	0.1016	0.0508
5	Insulation	0.0002	0.1020	0.0510
6	HTS Shield	0.0020	0.1060	0.0530
7	Neutral Conductor	0.0095	0.1250	0.0625
8	LN2 OUT	0.0026	0.1302	0.0651
9	Inner Cryostat	0.0099	0.1500	0.0750
10	Outer Cryostat	0.0030	0.1560	0.0780
11	Mantel	0.0050	0.1660	0.0830

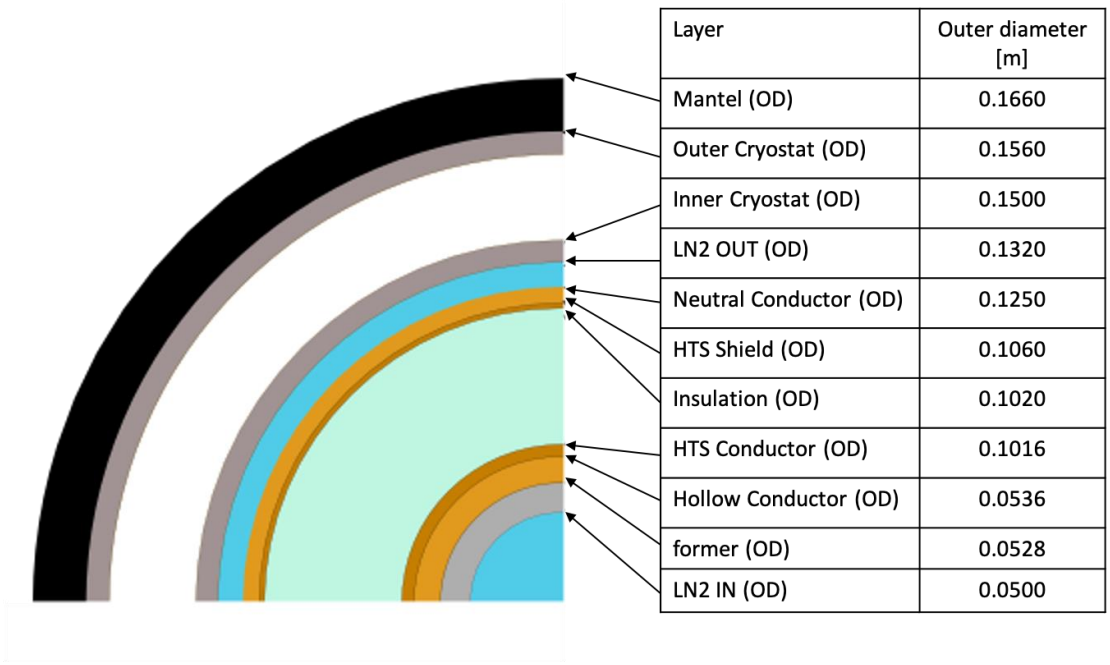

Figure 5. 5: Summary of cable geometry for HC DN50

Moreover, the design model provides the repartition of tapes in the HTS conductor and shield layer, represented in Table 5.9, where the length of tape material is given for single cable core:

Table 5. 9: CT DN50 cable's HTS tape repartition per core

HTS layer	Tape layer	Number of tapes in layer	Layer thickness [m]	Total tape length [km]	Tape length per km [m]
HTS Conductor	Layer 1	40	0.002	265.03	82.82
	Layer 2	40	0.002		
HTS Shield	Layer 1	77	0.002	255.09	79.72

5.3.3.2 Hydraulic Results

This configuration complies with the set operational temperature range that sits between 3 bar and 15 bar. Since hydraulic model created does not make a difference between former concepts, the pressure profile along the length of the cable is the same as in the Hollow Conductor former thus, shown in Figure 5.3. Table 5.10 also reproduce the same values as int the Hollow Concept.

Table 5. 10: DN 50 CT cable's key pressure points

Pressure at inlet of "cold" nitrogen [bar]	Pressure at warm/cold transition [bar]	Pressure at outlet of "warm" nitrogen [bar]
15.000	13.604	8.729

5.3.3.3 Thermal Results

The configuration respects the set thermal operational range for liquid nitrogen. Figure 5.6 displays the temperature of the liquid nitrogen flowing inside the former.

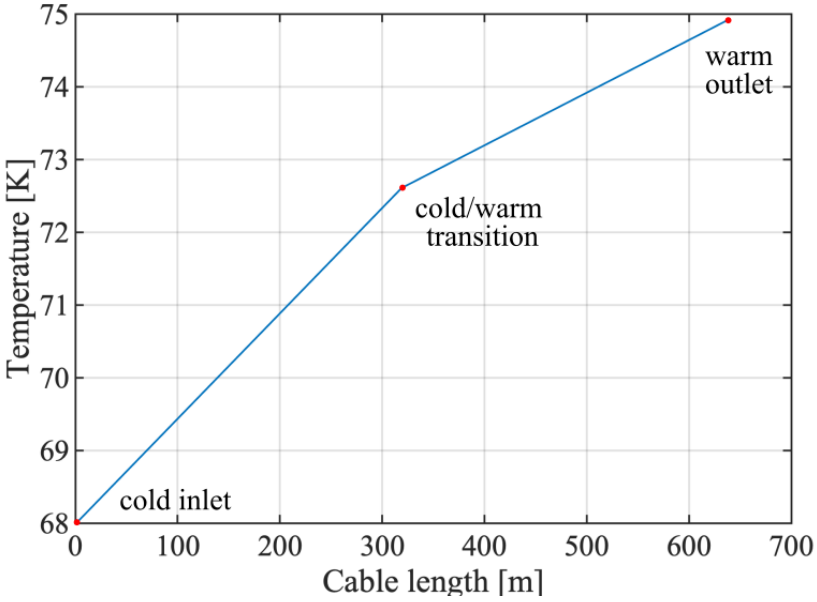

Figure 5. 6: CT DN 50 cable's Liquid nitrogen thermal profile

Table 5. 11: DN 50 CT cable's key thermal points

Layer	Temperature at "cold" inlet [K]	Temperature at cold outlet [K]	Temperature at "warm" inlet [K]	Temperature at "warm" outlet [K]
Liquid Nitrogen	68.000	72.620	72.620	74.931
HTS Conductor	68.015	68.291	72.630	72.768
HTS Shield	68.836	69.401	73.451	73.733
Cable's Maximum Global Temperature			**75.761 K**	

As it can be seen in the figure and table above, the temperature of liquid nitrogen is far from the 78 K maximal operational temperature, assuring the feasibility of the design. Moreover, the maximum global temperature of the cable is also under the set operational temperature range.

5.3.3.4 Losses

Table 5.12 contains the losses computed by the program:

Table 5. 12: Cable system losses for the DN 50 CT former

AC losses	1.445 kW
Current Lead losses	1.944 kW
Dielectric losses	5.712 kW
Line Cryostat losses	24.960 kW
Termination Cryostat losses	0.240 kW
Total System Losses	**34.301 kW**

CHAPTER 6 – ANALYSIS OF RESULTS

As seen in the last chapter, only two out of the six possible designs fulfill the requirements. This outlines the importance of the pressure and temperature checks. Moreover, it is also helpful to see how a cable configuration can be viable for some cases and not for others: if the case study where to be a two-sided cooling where "cold" liquid nitrogen flows through each of the phases, DN 32 and DN 40 configurations would have been feasible as the pressure boundaries would have been respected (results not reported here for the sake of conciseness).

On the other hand, both cable configurations with DN 50 formers have proven to be feasible. In this chapter, the difference between these 2 cable configurations will be further analyzed.

6.1 LAYOUT

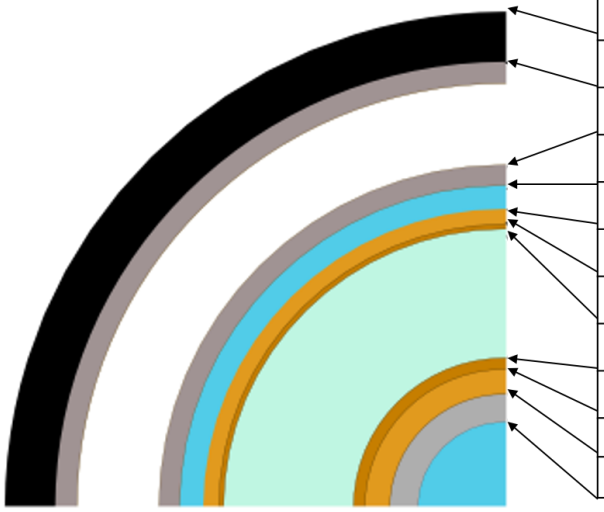

Layer	CT [m]	HC [m]
Mantel (OD)	0.1660	0.1660
Outer Cryostat (OD)	0.1560	0.1560
Inner Cryostat (OD)	0.1500	0.1500
LN2 OUT (OD)	0.1320	0.1320
Neutral Conductor (OD)	0.1250	0.1250
HTS Shield (OD)	**0.1060**	**0.1107**
Insulation (OD)	**0.1020**	**0.1067**
HTS Conductor (OD)	**0.1016**	**0.1063**
Hollow Conductor (OD)	**0.0536**	**0.0578**
former (OD)	**0.0528**	**0.0574**
LN2 IN (OD)	0.0500	0.0500

Figure 6. 1: Outer Diameter Geometry DN 50 Hollow Conductor vs Corrugated Tube

The thickness difference depends on the former choice. This occurs because the different former types present different thicknesses and, depending on the outer diameter of the Hollow Conductor layer, the HTS conductor tapes will have to be distributed in different number of layers. Looking back at the geometric results of each cable, we can see that there are different layers of HTS conductor in each of the configurations.

Table 6. 1: Comparison HTS Conductor tapes between former types

Cable Configuration	HTS cond. layer	Number of tapes in layer	Layer thickness [m]	**Total tape length [km]**	Tape length per km [m]
CT DN50	Layer 1	40	0.002	**265.03**	82.82
	Layer 2	40	0.002		
HC DN50	Layer 1	43	0.002	**142.45**	44.53

The electrical requirement of HTS tapes is the same for both configurations (43 tapes) but, since their geometry is different, the final number of tapes imposed on each configuration will be different. Because the Hollow Conductor former is thicker, it can house more tapes than the Corrugated Tube. In this case, the geometry of the Hollow Conductor allows to house all 43 tapes in one layer, while the smaller corrugated tube geometry only allows 40 tapes per layer, forcing to add a second 40-tape layer to fulfil electric requirements.

Table 6. 2: Comparison HTS Shield tapes between former types

Cable Configuration	HTS shield. layer	Number of tapes in layer	Layer thickness [m]	**Total tape length [km]**	Tape length per km [m]
CT DN50	Layer 1	77	0.002	**255.09**	79.72
HC DN50	Layer 1	80	0.002	**265.03**	82.82

In the shield, only geometrical tape requirement is considered. However, because the Hollow Conductor takes up more space, the tapes needed to cover the surface of the insulation is greater thus, requiring more tapes for the shield compared to the Corrugated Tube former.

6.2 TEMPERATURE

The temperature of the Corrugated Tube (CT) is expected to be lower compared to the Hollow Conductor (HC) because it has more tapes and layers, meaning that each tape is carrying less current and thus the tapes produce less AC losses, leading to a lower temperature.
In reality, we can see that indeed, the CT temperature is higher, but the difference in temperature profiles of liquid nitrogen between the two former types is negligible after simulating the profiles with the model (see Figure 6.2).

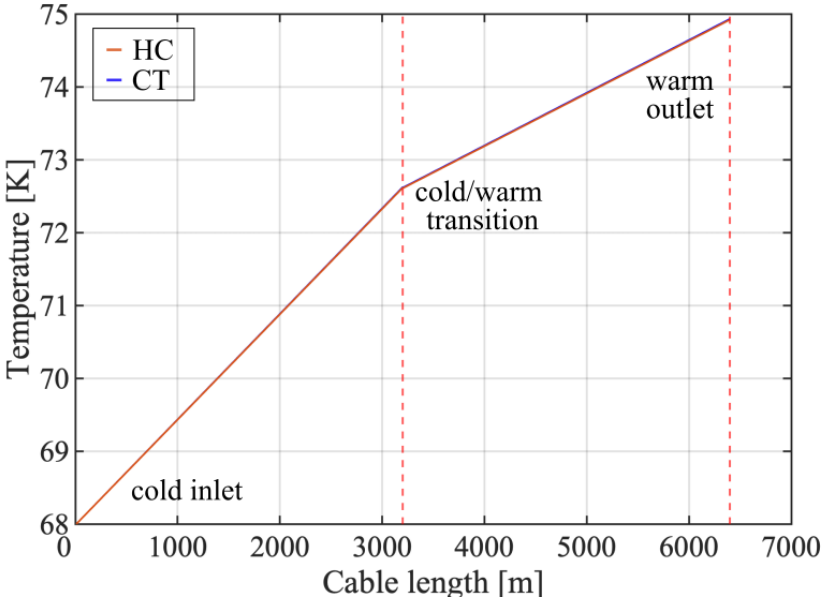

Figure 6. 2: LN2 Temperature profile comparison

6.3 LOSSES

It is in the losses model and results where one can see the impact of the choice in former type.

Table 6. 3: Losses comparison DN50 Hollow Conductor vs Corrugated Tube

	HC DN50	CT DN50
AC losses	10.022 kW	1.445 kW
Current Lead losses	1.944kW	1.944 kW
Dielectric losses	5.995 kW	5.712 kW
Line Cryostat losses	29.960 kW	24.960 kW
Termination Cryostat losses	0.240 kW	0.240 kW
Total System Losses	**43.161 kW**	**34.301 kW**

The most noticeable difference in losses can be seen in the AC losses of the cable. There is a reduction of 86% of the AC losses between the Hollow Conductor and Corrugated Tube former types. The rest of the losses either suffer no changes as they are geometry-independent or, like the dielectric losses that only decrease 5%, have no significant impact on the total loss account.

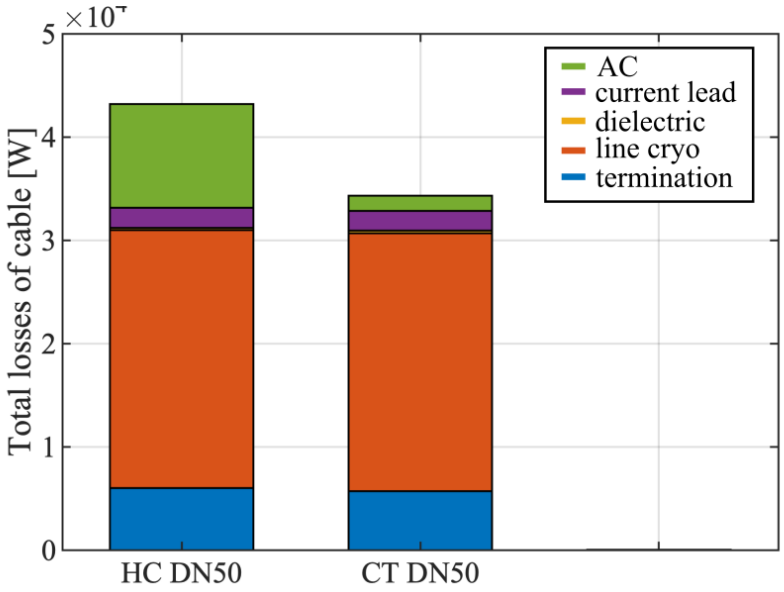

Figure 6. 3: DN50 total loss comparison between former types

The AC loss difference between former types can be explained by the difference in the cable geometry: the Hollow Conductor concept has just one layer of 43 tapes in the HTS conductor layer while the Corrugated Tube has two layers of 40 tapes each. The nominal current is carried evenly by all the tapes composing the system, meaning that the tapes in the Hollow Conductor concept will be supporting a greater current than those in the Corrugated Tube.

Table 6.4 shows the ratio $k = \frac{I_{carried\ by\ tape}}{I_c}$ for all the six possibilities, where the current carried by each type is the nominal current divided by the total number of tapes on the HTS conductor layer/s.

Table 6. 4: Ratio k of current carried by tapes

	DN32	DN40	**DN50**
HC	0.387	0.333	**0.558**
CT	0.462	0.375	**0.300**

The results shown above demonstrate that the proportion of the nominal current carried by the Corrugated Tube at DN 50 is significantly lower than that of the Hollow Conductor for the same diameter. Moreover, through equations (18) and (20) of the losses model it can be clearly seen that the AC losses depend directly on the ratio k.

6.4 ECONOMIC CONSIDERATIONS

The Capital Expenditure or CAPEX is the one-off expenditure that results in the acquisition, construction or enhancements of significant fixed assets including land, buildings and

equipment that will be used or benefited from for more than one financial year, while the Operational Expenditure or OPEX, is the expenditure incurred as the result of the day-to-day operations of a business or installation such as wages, utility and maintenance costs, repairs, rand rent [INST21].

In the case of the superconducting cable system, the CAPEX are all costs regarding the installation and material cost of the system, while the OPEX will be the maintenance costs and the refills of liquid nitrogen.

The CAPEX is directly impacted by the HTS tape length. The HTS tape length for the 6 cable configurations was calculated and plotted them on Figure 6.4. It demonstrates that the required total length of HTS tapes is a function of both the DN and former type. Note that the corrugated tube configuration does not always require more conductor than the hollow conductor concept. While it is true that DN32 and DN40 configurations are not feasible for the considered case study, they may be feasible for other applications. This illustrates how the geometry affects HTS material quantity.

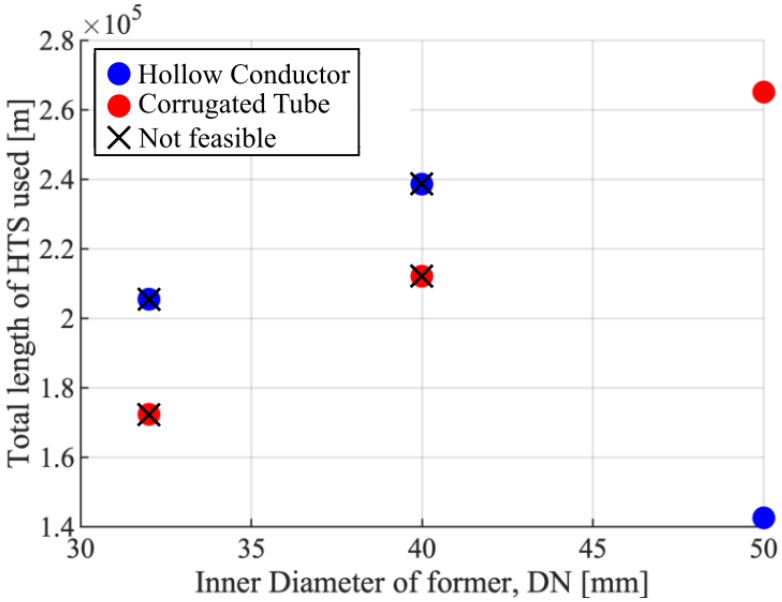

Figure 6. 4: Total quantity of HTS material as a function of DN and former type for the studied case.

Indeed, the quantity of HTS tapes needed to build a superconducting cable system is a key factor in the decision process because it directly impacts the capital expenditure of the project (CAPEX). The price of an YBCO coated 4 mm tape having an I_c of 150 A varies between 25 and 100 €/kA·m. For the considered case study, the choice of the former type leads to a CAPEX difference of up to 2.5 million euros.

Table 6. 5: HTS material cost comparison for YBCO, I_c=150 A tapes

	HTS tape length per core [km]	Total HTS tape length per cable system 2x3ph [km]	**Total Cost @25 €/kA·m [€]**
HC DN50	407	2445	**9,168,300**
CT DN50	520	3121	**11,702,700**

The OPEX is directly related to the cable losses. We calculated the losses for the 6 cable configurations and plotted them in Figure 6.5.

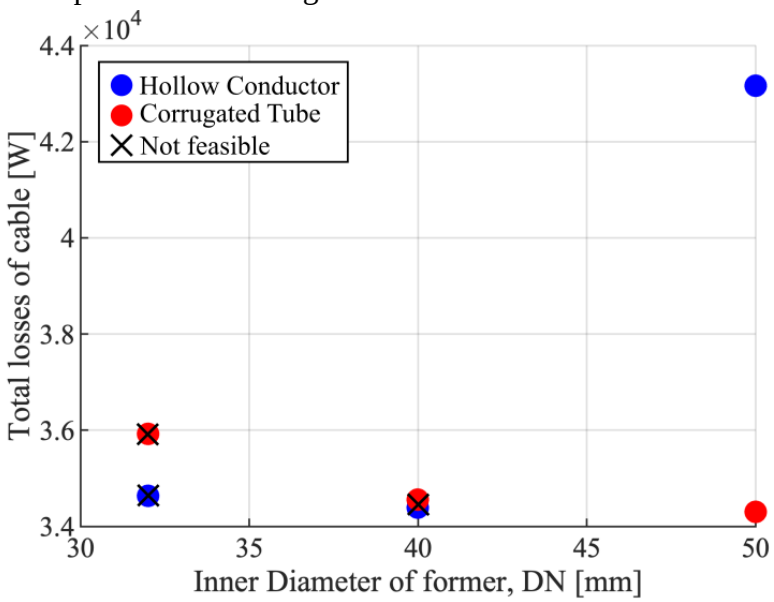

Figure 6. 5: Total Losses of system as a function of DN and former type (at nominal operation point)

Note that the objectives of minimizing the HTS tape length and cable losses are antagonistic. The designs that contain more HTS tapes are those that generate fewer losses.
The reason behind this phenomenon has already been explained in the comparison of losses made in the previous section. Like in the quantity of HTS material, the quantity of generated losses is also a key factor in the designing process as it directly impacts the overall efficiency of the system and thus on the economic performance of the network and operational costs (OPEX).

Considering the results, there is no direct answer to which cable configuration should be selected. One of the feasible options is the most cost competitive regarding the initial investment while the other proves to be the most cost competitive during operation, meaning that the program does not give a direct solution on which cable must be installed, but it provides the user with all the required knowledge for him to make a compromise between investment and operational costs and performance. Therefore, to go further, an economic model should be included.

CHAPTER 7 – EXPERIMENTAL WORK

The other objective of this work to contribute to the standardization of superconducting cables by creating a testing station and protocols at the laboratory in order to make it possible to fully characterize a superconducting cable core.

7.1 HTS TAPE MEASUREMENT PROTOCOL

We proceeded to the establishment of an in-house protocol that follows national and European standards to measure superconducting materials.

The protocol is made specifically for measuring individual superconducting tapes as they are the elementary component of the superconducting cable.

The aim of the protocol is to measure the current-voltage characteristic of the tapes and to deduce the tape's critical current. To do so, several tests were carried out on different types of superconducting tapes throughout the year, adapting and improving the protocol at each new test while verifying it to the European standard [ISSN03] for superconducting tape measurement.

7.1.2 PROTOCOL CONTENT

Devices

- Current Source: *Sorensen SGX Series Programmable Precision High Power DC Supply.*
- Nano-voltmeter: *Keithley Nanovoltmeter 2182A* .

Superconducting tape sample

- Total length, L = 15 cm
- Measured length, L_{sample} = 10 cm

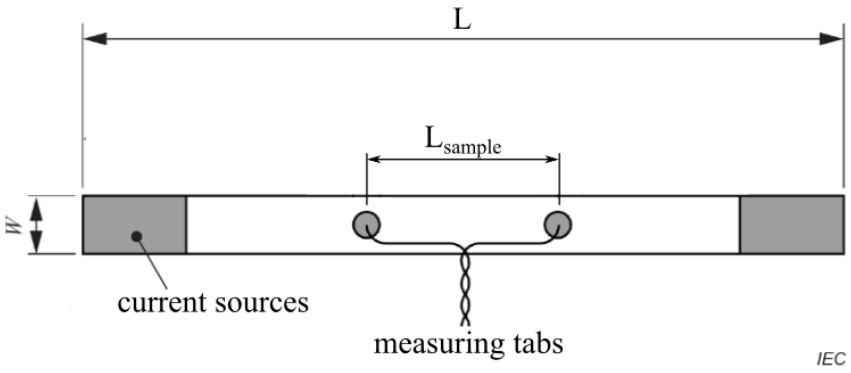

Figure 7. 1: Diagram of sampled tape

Testing Principle

The protocol lays down the groundwork for each step of the measuring experiment. From explaining how the tape should be prepared to how to connect the current source and the nanovoltmeter to perform the measurement and how to deal with the liquid nitrogen. The detailed superconducting tape measurement protocol.

To find the critical current of the tape, [ISSN03] states that the critical current is that corresponding to 10 $\mu V/cm$. For the 10 cm of tape length defined in the protocol, this means that the critical current corresponds to a voltage of 10 μV. A first test is performed by augmenting the current in steps of 10 A until the 10 μV mark is reached to approximately locate the critical current of the tape and then it is stopped to prevent the tape from being damaged.

A second test is then performed in steps of 5 A and 2 A to measure the I-V characteristic until the tape quenches or breaks. This second, more detailed test is the one that is used as the I-V characteristic and to determine the critical current of the tape.

The protocol then provides a post-processing code to plot the I-V characteristic and find the critical current correctly, while eliminating offsets.

7.1.2 EXAMPLE OF RESULTS

If the protocol is correctly followed, the I-V characteristic and the critical current of the tape can be obtained experimentally. In this section, one of the many tests carried out to construct and test the protocol is shown.

Figure 7.2 shows the I-V characteristic obtained for a Sumitomo BSCCO superconducting tape, it can be clearly seen that the voltage of the tape is negligible up to the critical current, I_c.

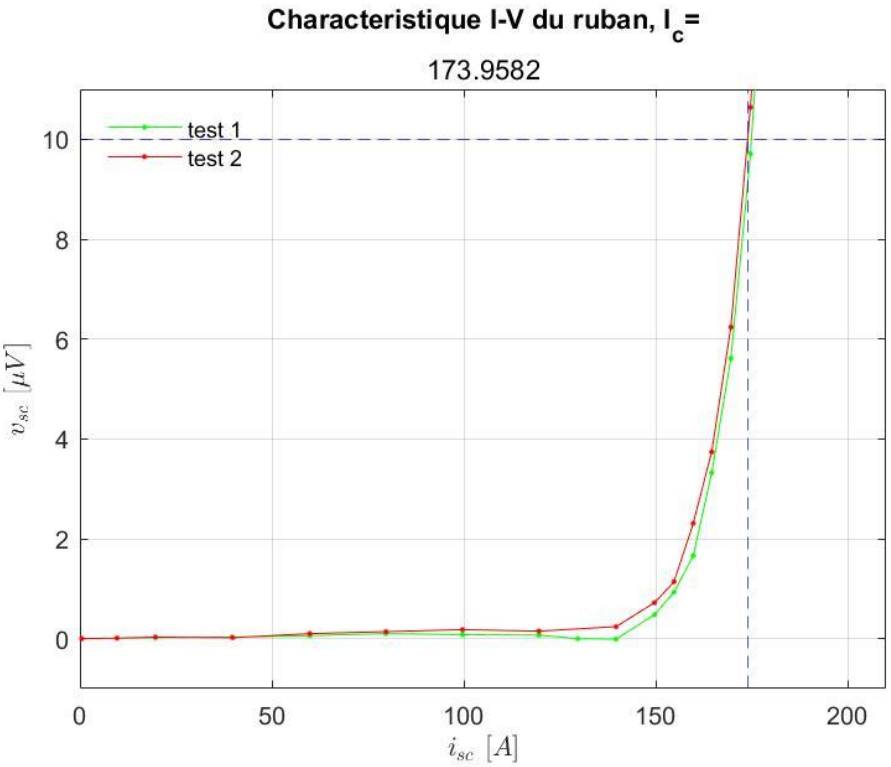

Figure 7. 2: I-V characteristic for Sumitiomo_BSCCO_HTCA_CETS_2019_068_001 tape

To accurately determine the critical current of the tape model, several tests are carried out on the same type of tape and compared (see Figure 7.3).

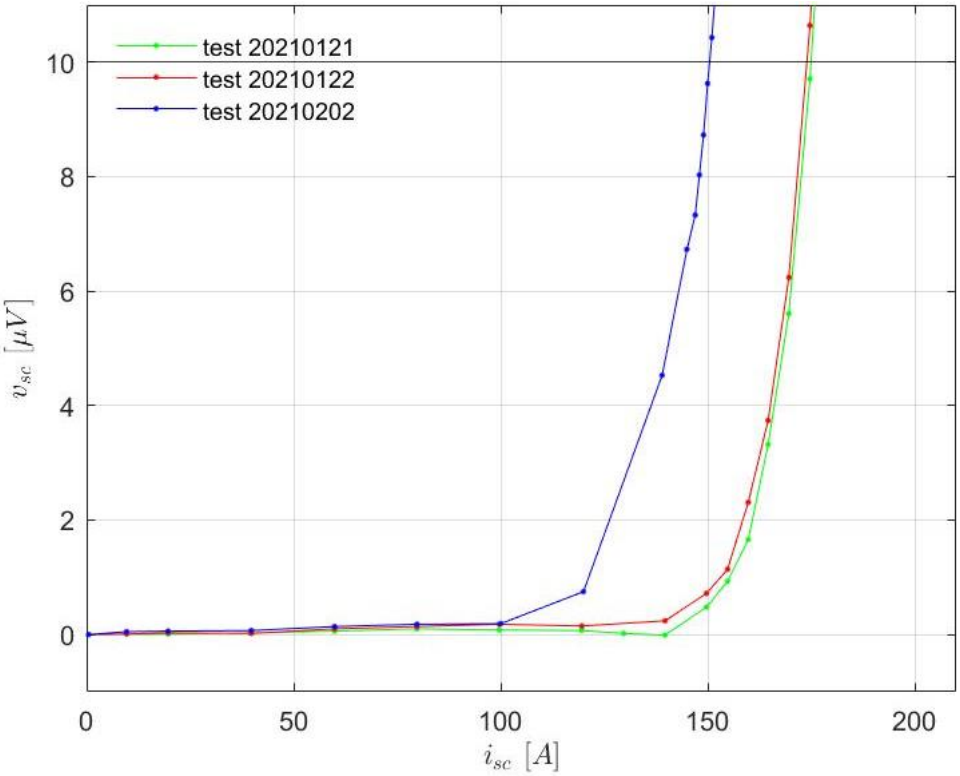

Figure 7. 3: Comparison of I-V characteristics for Sumitiomo_BSCCO_HTCA_CETS_2019_068_001 tapes

Table 7. 1: Critical currents of the tapes presented on Figure 7.3

Test	Critical current, I_c $[A]$
20210121	174.96
20210122	173.95
20210202	150.46

Because of the comparison of the profiles obtained in different tests we can see that the tape corresponding to the 20210202 test must have been damaged during handling, resulting in a lower critical current compared to the other two measurements. Note that the theoretical critical current of a Sumitiomo_BSCCO_HTCA_CETS_2019_068_001 is $I_c = 170\ A$.

7.1.3 FUTURE PERSPECTIVE

In the future, the protocol will be adapted for the measurements of superconducting cables. Before extending the protocol to greater lengths, it is essential to automatize it, since in the current version it is the user who must increase the current in the source and note down the voltage from the nanovoltmeter.

Once the process has been automatized, since a superconducting cable is essentially composed of twisted superconducting tapes in parallel, the logical order should be to adapt the protocol for parallel tapes, and then develop a procedure to measure all the tapes of a cable simultaneously.

7.2 CONSTRUCTION OF A TEST STATION

The construction of the test bench has as its main goal to be able to perform tests on the cable core owned by GeePs. Figure 7.4 shows the cable core for which the specifications are as follows:

- T = 77 K
- L = 2 m

Figure 7. 4: 2 m cable core

The objective is to construct the test bench shown in Figure 7.5. A polystyrene cryostat is used to keep the liquid nitrogen bath at 77 K. Copper connectors are welded at each of the extremities of the cable core. The connectors are connected thanks to two current braids (Figure 7.6) to the sources.

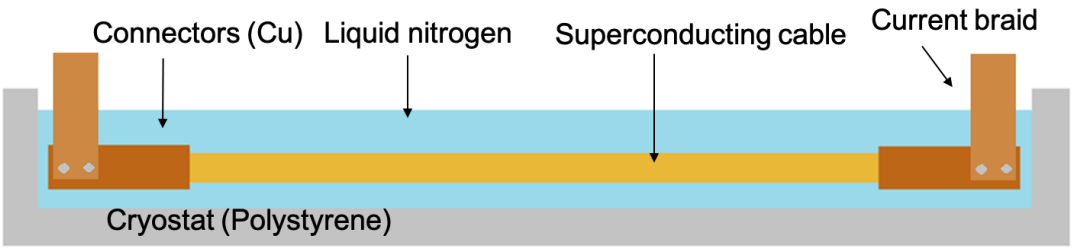

Figure 7. 5: Testing facility to be developed

Out of the components outlined in Figure 7.5, the copper connectors and the polystyrene cryostat have been manufactured as part of this work. In the sections to come, the manufacturing process of these elements is explained.

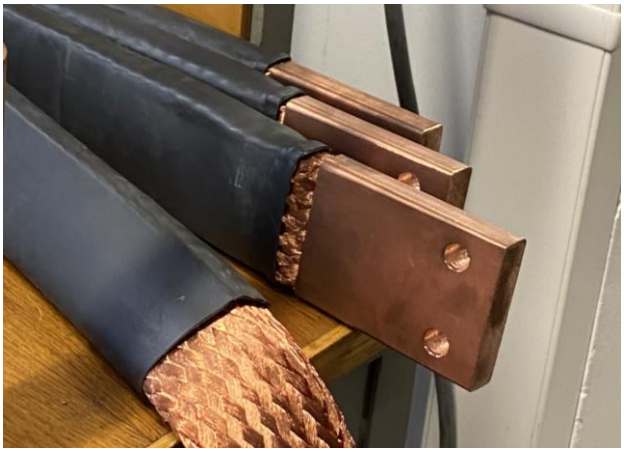

Figure 7. 6: Current braids

7.2.1 POLYSTYRENE CRYOSTATS

Commercial cryostats have been described in Chapter 2. For the test station, the studied cable has only a length of 2 m, it is not necessary to have a perfect insulation nor a pumping system to achieve a nitrogen flow through a pipe. Also, the fact that the tests won't be carried out over long periods of time means that a perfect insulation is not needed, but just one that slows liquid nitrogen evaporation enough so that measurements can be taken.

The proposed solution for the cryostat is a dense polystyrene container, with a cavity big enough to house the cable core. For the fabrication, a 2.5 m dense polystyrene block was ordered. The key to fabricating the cryostat was to carve a uniform cavity inside the block. To do so, first the profile to be cut was drawn in the block (Figure 7.7) and then, the cavity had to be carved.

Figure 7. 7: Polystyrene block to be carved

To do so, a polystyrene-cutting system had to be developed. The solution was to braid a heating wire with itself in the shape desired for the cavity. The braided cable was then attached to a sturdy base so we could operate it without the risk of burning ourselves. Then, the wire was connected to a current source and was left heating up until it was hot enough to cut the polystyrene clean. In Figure 7.8, the device used to cut out the cryostat is showed.

The key to carving the cavity was to keep the wire still while pushing the polystyrene block. It was a long process that then required filing the sides and end of the cavity to have smooth and uniform surfaces. Figure 7.9 shows the result.

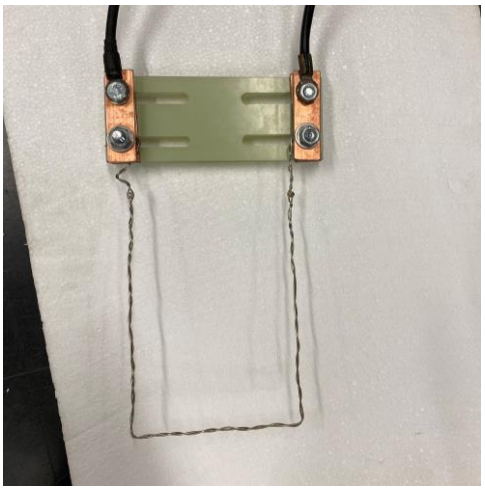

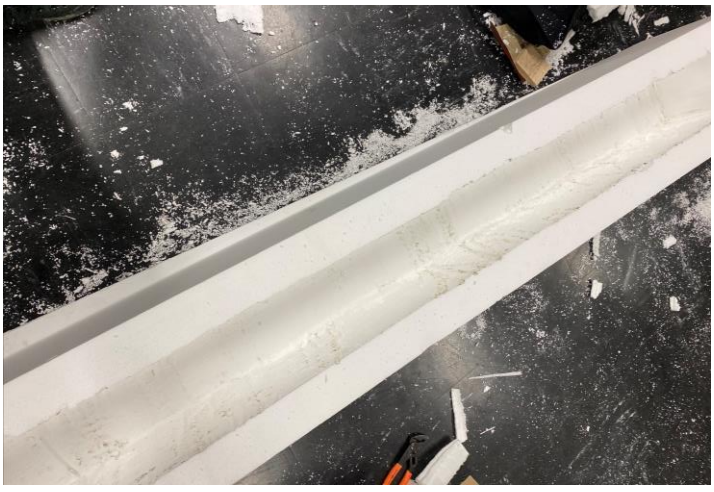

Figure 7. 8: Heating wire

Figure 7. 9: Result for cryostat

7.2.2 COPPER CONNECTORS

The function of the copper connectors is to carry out the current from the cable core to the current braids since they cannot be directly connected to the cable. The connectors must be hollow so the extremities of the cable can be inserted and welded to it. In Figure 7.10 the preliminary CAD design of the connectors is shown. Figure 7.11 shows the connector welded to a test cable piece while Figure 7.12 illustrates how the connector can be attached to the current braid.

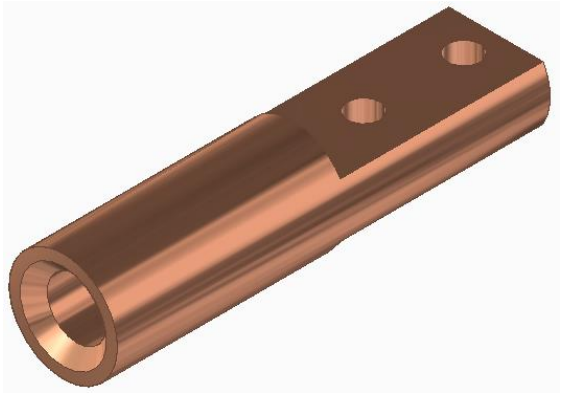

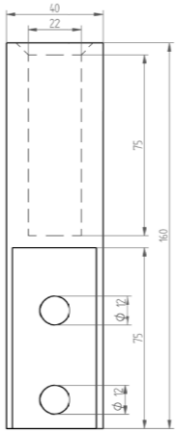

Figure 7. 10: CAD design of copper connectors

Figure 7. 11: Welded connector

Figure 7. 12: Connector and current braid

7.2.3 WELDING CONNECTORS TO CABLE

Because the HTS conductor tapes are brittle and can be damaged by the heat, a specific welding protocol had to be developed to weld the ends of the cable core to the copper connectors. In this section, the established protocol is detailed with illustrative images of the welding of a test cable to a test connector.

1- Take the cable core and carefully remove and cut the protective milar layer up to 11 cm of length. See Figure 7.13a)
2- If the tapes don't open in a plume, separate them carefully and remove the adhesive layer that keeps the tapes together so that the cable core resembles to the one in Figure 7.13b)
3- Start removing the Kapton protective layer for each tape separately. To ensure the protection of the superconducting material, first start removing the Kapton of the inner layer and then the outer one. When all the Kapton is successfully removed, the core must resemble Figure 7.13c).

a) Removing Milar *b) Removing Adhesive* *c) Removing Kapton*

Figure 7. 13: Removing protective layers

4- Once all tapes are exposed, relocate them in their original, twisted position and fix them in place using a copper thread. Tight the copper thread to ensure that the tapes are kept in place. If necessary, use an adhesive tape in the end. See Figure 7.14a).
5- To make the welding possible, it is necessary to use a heating collar around the connector to raise its temperature. The heating collar's temperature is regulated by the electronic system shown in Figure 7.14b).
6- Install the heating collar around the connector and connect the collar to the electronic regulator. Fix the connector in a vertical, upright position as shown in Figure 7.14c)

with the help of the vice. Verify that the collar-connector system is stable before proceeding.

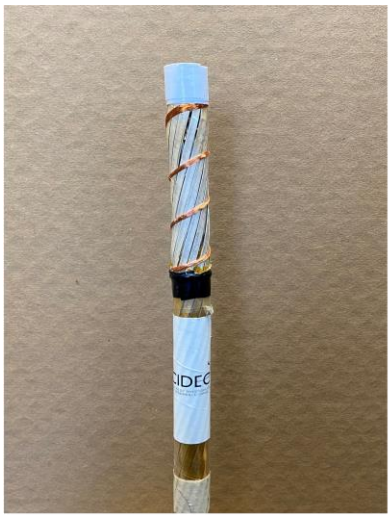

a) Prepared cable core

b) Electronic temperature regulator

c) Welding setup

Figure 7. 14: Steps 4 to 6

7- Before heating the connector, clean the cavity using flux (Ref: BS10) as shown in Figure 7.15a). To perform this step, put on the corresponding personal protective equipment (gloves and face mask to prevent inhalation of vapors).
8- Start to heat the connector and monitor the temperature raise with the thermal camera. See Figure 7.15b)
9- When the connector reaches a temperature of 140°C insert the lead-tin alloy (nº7439-92-1) with tweezers and protective gloves and wait for it to melt. Repeat this process until two thirds of the cavity is filled with melted lead-tin. See Figure 7.15c)

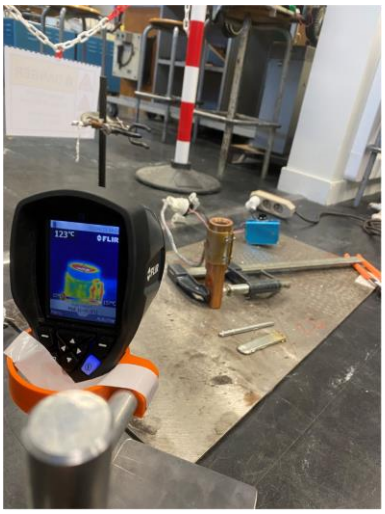

a) Cleaning connector with flux *b) Connector's temperature* *c) Melting lead-tin alloy*

Figure 7. 15: Steps 7 to 9

10- Make sure that the melted lead-tin alloy sticks to the walls of the cavity, even for the part that is not filled with the melted alloy. It is essential to have good electrical contact with the cable. See Figure 7.16a).
11- Monitor the temperature with the camera, ensuring it stays below 190°C (greater temperatures would harm the HTS material) but making sure that the connector is hot enough to keep the lead-tin bath in liquid state. See Figure 7.16b)
12- Once the appropriate temperature is reached, install the cable on the clamp as shown in Figure 7.16c), carefully aligning it with the connector's cavity. Carefully slide down the cable through the clamp to insert it inside the connector

a) Lead-tin bath *b) Monitoring bath temperature* *c) Cable setup for welding*

Figure 7. 16: Steps 10 to 12

13- Apply pressure on the cable to ensure that the cable reached the bottom of the connector's cavity. Once the cable rests on the bottom, turn off the heating collar and leave it to cool down so the welding solidifies. Make sure that the system is at room temperature before disassembling the setup.
14- Once the connector is cold, remove the heating collar and verify that the joint is solid. The welding process has finished, 7.17a) and b) show the result.

a) Colling the joint

b) Finalized joint

Figure 7. 17: Welding Result

7.2.4 ASSEMBLY OF THE TESTING FACILITY

After all the components listed above have been either manufactured or purchased, the final step is to prepare the cable so it can be tested. To do so, the welding protocol listed in the previous section is applied to weld both ends of the cable core to their corresponding connectors. Images showing the different steps of the welding protocol were followed are shown in Figure 7.18.

a) Step 1

b) Step 2

c) Step 3

Figure 7. 18: Welding the cable

Because the cable core is very susceptible to damage when moved, it was key to keep it upright throughout the whole welding process. Thus, the cable had to be suspended from the ceiling to keep it vertical and lower it slowly to weld it to the connector. See Figures 7.19 to 7.20.

a) Step 4 *b) Step 4* *c) Step 6*

Figure 7. 19: Welding the cable

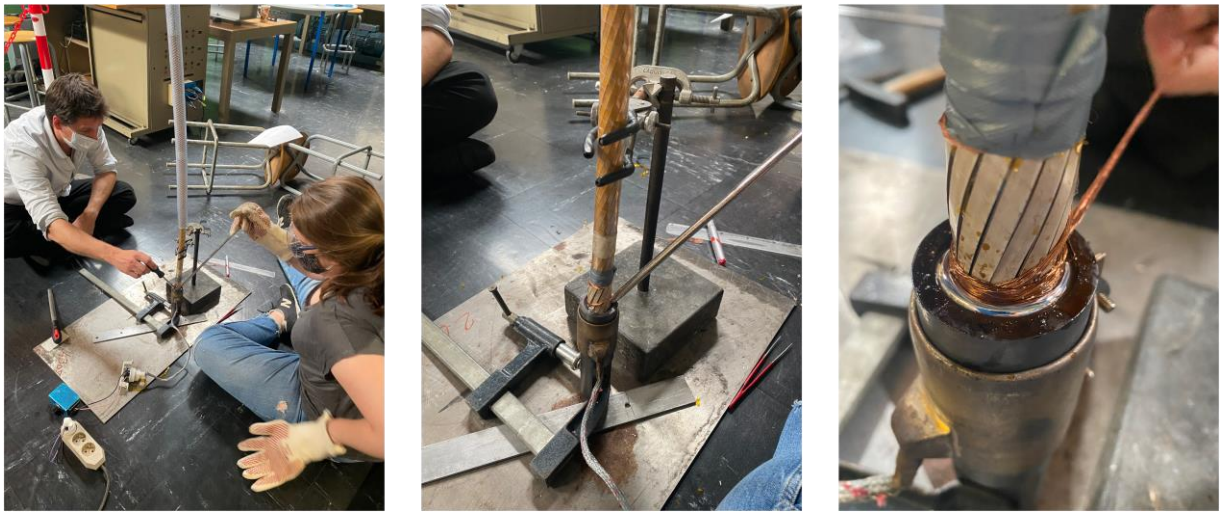

a) Step 9 *b) Step 12* *c) Step 13*

Figure 7. 20: Welding the cable

In the images 7.20 b) and c) we can see how the lead-tin alloy makes the electric contact between the external tapes of the cable core and the connector. After step 13 of the welding protocol was achieved, the heating collar was turned off and the cable core and connector were left to cool for an hour. The welding process was performed twice, once for each cable core and connector.

After both connectors were properly welded, it was time to install the cable in the cryostat.

Because the superconducting tapes are susceptible to damage with any sort of movement, it was essential to ensure that the cable stayed stable at the bottom of the cryostat. To do so, some polystyrene cryostats were created, having the circular profile of the cable carved for the core would fit perfectly inside them. Their mission is to support the weight of the cable, so it does not curve due to its own weight. The spacers are shown on Figure 7.21.

Figure 7. 21: Cable core resting on spacers

Once the spacers were completed, they were fixed to the bottom of the cavity of the polystyrene cryostat. Then, the cable was carefully inserted in the spacers and the connectors were bolted to the current braids.

Figure 7. 22: Cable core installed inside cryostat

Figure 7. 23: Current braid bolted into cable core + connector system

7.2.5 STEPS TO COME

Due to the health crisis suffered during the development of this project, the access to the laboratory was limited and not all the intended experimental work could be completed and therefore, the test station could not be used to perform a test on the superconducting cable core. The following steps will be performed in the future and are necessary for the completion of the test station:

- Welding the measuring tabs to the connector so they can be connected to the nanovoltmeter to measure the potential difference between the ends of the cable core.
- A protection system using diodes must be developed to protect the very expensive current sources in case of a current fault.

CHAPTER 8 – CONCLUSION

The aim of this project was to contribute to the standardization of superconducting cables.

Throughout the development of the project, we created a framework for the design of a superconducting cable system. Although the framework does not yet cover all possibilities of HTS cable configurations, its application to the 1 core 1 cryostat configuration allowed us to obtain results that complete previous works. The current framework could easily be expanded to cover more possibilities and used within an optimization routine.

On the experimental side, a protocol to standardize the measurement of the I-V characteristic of a superconducting tape was developed. Using the same measurement protocol can unify the results of different tests and manufacturers, providing a more reliable and accurate way to compare results between different experiments. Finally, the construction of a superconducting cable test station participates in the development of advanced test equipment at GeePs laboratory, as it will allow to test superconducting cables, not relying on third-party facilities and thus be a step forward in the analysis and development of superconducting cables.

BIBLIOGRAPHY

[CDEN14] Connaissance des Énergies: 'Combien de pertes de ligne en France', 2014. Available: https://www.connaissancedesenergies.org/electricite-a-combien-s-elevent-les-pertes-en-ligne-en-france-140520

[MERS13] Merschel, F., Noé, M. T&D World: 'The AmpaCity project'. December 23, 2013. Available: https://www.tdworld.com/overhead-distribution/article/20964180/the-ampacity-pro

[SCHM05] Schmidt, F., Allais, A. Workshop on accelerator magnet superconductors: 'Superconducting cables for power transmission applications'. Hannover, 2005.

[NOE_17] Noé, M. EUCAS Short Course on Power Applications: 'Superconducting Cable', Geneva, 2017.

[MUKO17] Mukoyama, S., Yagi, M. IEEE Transactions on Applied Superconductivity: 'Experimental Results of a 500 m HTS Power Cable field Test'. Pp 1680-1683. 2017.

[ICHI07] Ichikawa, M., Torii, S. IEEE Transactions on Applied Superconductivity: 'Quench Properties of 500-m HTS Power Cable'. 2007.

[HYUN09] Hyung, S.Y., Dong L.K. IEEE Transactions on Applies Superconductivity: 'Long Term Performance Test of KEPCO HTS Power Cable'

[NOE_13] Noé. M. Foestering Collaborations in Superconductivity: 'Superconductivity as a key technology from small electronics to large magnet applications'. Madrid, 2013.

[TIXA10] Tixador, P. Physica C, Supercondcutivity and its Applicatios: 'Development of superconducting power devices in Europe'. Pp 971-979. 2010.

[SYNT09] Synikov, V.E. IEEE Transactions on Applied Superconductivity: '30 m HTS Power Development and Witness Sample test'. Pp 1702-1705. 2009.

[MAGU10] Maguire. J., Folts, D. Advancements in Cryogenic Engineering: 'Status and Progress of a fault limiting HTS cable to be installed in the con Edison grid'. 2010.

[MELN09] Melnik, I. Geschiere, A. EUCAS 09: 'Long-term HTS cable with integrated FCL property'. 2009.

[RAIN11] Rainer, S., Granados, X. IEEE Transactions on Applied Superconductivity: 'ENDESA Supercable, a 3.2 kA 138 MVA MTS power cable'. pp972-975. 2011

[YOUN07] Jae-Young, Y., Seung, L. IEEE Transactions on Applied Superconductivity: 'Application methodology for 22.9 kV HTS Cable in Metropolitan City of South Korea'. Pp 1656-1659. 2007.

[SYNT15] Synikov, V.E., Bemert, S.E. EEE Transactions on Applies Superconductivity: 'Status of HTS cable Link Project for ST. Petersbourg Grid'. 2015

[STOV11] Stovall, J.P., Demko, J.A. IEEE Transactions on Applied Superconductivity: 'Installation and Operation of the Southwire 30-meter HTS Power Cable'. vol 1. No.1. pp 2467-2472. 2011

[WILL02] Willen. D, Hansen, F. Physica C 372-376: 'First operation experiences from a 30 kV, 104 MVA HTS poewer cable in a utility substation'. ELSEVIER. Ppp 1571-1579. 2002.

[TONE04] Tonnensen. M. Superconductor Science and Technology: 'Operation Experiences with a 30 kV/100 MVA HTS cable system'. 2004.

[YXIN04] Xin, Y., Hou, B. Superconductor Science and Technology: 'China's 30 m 35 kV/2 kA AC HTS power cable project'. Vol 17. Pp 332-335.

[DEMK06] Demko, J.A., Duckworth, R.C. AIP Conference Proceedings: 'Testing of a liquid nitrogen-cooled 5-meter, 3000 A Tri-axial HTS Cable system'. 2006.

[LINS08] Linsday. D., Roden, M., CIGRE: 'Operating Experience of 13.2 kV superconducting cable system at AEP bixby station'. 2008.

[YUMU09] Yumura, H., Ashibe, Y., IEEE Transactions on Applied Superconductivity: 'Phase II of the Albany HTS Cable Project'. Pp 1698-1701. 2009

[SCHM12] Schmidt, F., Maguire, J. Physics Procedia, Superconductivity Centennial Conference: 'Operation, Experience and Further Development of an HTS Power Cable in the Long Island Power Authority Grid'. Elsevier 2012. Vol 36. Pp 1137-1144.

[SOHN12] Sohn, S., Yang, H. IEEE Transactions on Applied Superconductivity: 'Installation and Power Grid demonstration of a 22.9 kV, 50 MVA HTS Cable for KEPCO'. 2012.

[CHEO13] Cheolhwi, R., Hyunman, J. Proceedings of IEEE International Conference on ID3231 Applied Superconductivity and Electromagnetic Devices: 'Current Status of Demonstration and Commercialization of HTS cable system grid in Korea'. Beijing, 2013.

[MAGU11] Maguire, J.F., Yuan, J. IEEE Transactions on Applied Superconductivity: 'Progress and Status of a 2G HTS Power Cable to be Installed in the Long Island Power Authority (LIPA)'. Vol. 21. No. 3. Pp 961-966. 2011.

[HIRO13] Hiroyasu, H., Ashibe, Y. IEEE Transactions on Applied Superconductivity: 'Update of Yokohama HTS cable project'. 2013.

[AMPA13] Proceedings of 2014 IEEE International Conference on Applied Superconductivity and Electromagnetic Devices: 'AmpaCity – Installation of Advanced Superconducting 10 kV System in City Center Replaces Conventional 110 kV Cables'. Beijing, 2013.

[GEON 20] Geon, L., Su, B. IEEE Transactions on Applied Superconductivity: 'Condition Monitoring of 154 kV Cable Systems via Temporal Sliding LSTM Networks'. 2020.

[KOTT19] Kottonau, D.; Shabagin, E.; de Sousa, W. 'Evaluation of the Use of Superconducting 380 kV Cable'. KIT Scientific Publishing, 2019.

[TPIN19] Triple Product Inc., Fusion Energy Base, 2019. Available: https://www.fusionenergybase.com/concept/rebco-high-temperature-superconducting-tape

[MASU15] Masuda, T., Yumura, H. SEI Technical Review: 'High-temperature Superconducting Cable Technology and Development Trends'. 2015

[CRYO12] Nexans, CRYOFLEX: 'Transfer Lines for Liquid Gases'. 2012.

[BURN18] Burns, B. History of the Atlantic Cable & Undersea Communications. December Available: https://atlantic-cable.com/Cables/Power/index.htm

[ISO_12] ISO 10380, DIN EN 10380. Pipes – Corrugated hoses and metal hose lines. 2012.

[MATH21] Mathweb.fr. 2021. Available: https://www.mathweb.fr/euclide/methode-darchimede-et-encadrement-de-pi/

[SOUS20] De Sousa, W.T.B., Kottonau, D., Noé, M. Superconductor Science & Technology: 'An Open-Source "A Finite Difference Based Transient Electro-Thermal Model for Superconducting Power Cables'. 2020.

[IEC_60] IEC 60287. 'Electric Cables – Calculation of the Current rating'. p. 33.

[CRYO15] Cryotherm: 'Cryo-Leitungssysteme'. 2015. p. 5

[HERR93] Herrmann, P.F:, Cotteveille, C. SIEMENS AG: 'Cryogenic Load Calgulation of high Tc current lead'. D_8520 Erlangen, Germany.

[KOTT17] Kotonau. D, Shabagin, E., Noe, M. IEEE Transactions on Applied Superconductivity: 'Oportunities for High-voltage AC Superconducting Cables as Part of New Long-Distance Transmission Lines'. Vol 17. No. 14. 2017

[INST21] Institute of Civil Engineers UK. Designing Buildings. Available: https://www.designingbuildings.co.uk/wiki/Capital_expenditure_for_construction

[ISSN03] ISSN0335-3931. Supraconductivité Partie 26: Mesurage du courant critique –Courant critique continu des composites supraconducteurs de RE-Ba-Cu-O. Norme Française.

ANNEX I – SOURCE CODE MAIN.M

```
% Carmen Martín-Sanz Garrido
% main script for a superconducting cable desing following the method of
% Noe17 and the model by D. Kottonau in his PhD thesis.

% from version 20210629: - number of cables not accounted for inside the functions, it is
% accounted for in the main.

% There are two cable configurations since we have one sided cooling:
% - CA: its inlet recieves LN2 from the source
% - CB: its inlet recieves LN2 from the outlet of two CA cables (has double
%       mass flow)

% Before running the file, add to path the files in the folder "thermique".

clear all, close all, clc
```

Cable Specifications

```
% parameters


% variables
dz = 10;                                %[m] axial discretization for thermal model, At dz=1
we have the most accuracy for loss computation but it takes longer to calculate. For
iterations dz=10 is reccomended
L_cable = 3200;                         %[m] cable length
Ir = 3600;                              %[A] rated current of one cable
Vn = 220e3;                             %[V L-N RMS] nominal voltage of cable
f = 50;                                 %[Hz] frequency
n_cable_CA = 4;                         %[-] number of cables with IN configuration
n_cable_CB = 2;                         %[-] number of cables with OUT configuration
delta_h = 0;                            %[m] height difference between inlet and outlet
mdot = 0.9;                             %[kg/s] flow rate of LN2 at inlet
T_in = 68;                              %[K] temperature of LN2 at inlet
DN = 50;                                %[-] former tube size = outer diameter LN2
former_type = 'CT';                     %[-] former concept: HC = hollow conductor, CT =
corrugated tube

% Superconducting tape physical parameters
alpha_drill = 15*pi/180;                %[rad] twist angle
k_SI = 0.8;                             %[A] current margin, btw 0.5 and 0.8
w_tape = 4e-3;                          %[m] tape width
T0 = 77;                                %[K] temperature SF
Ic = 150;                               %[A] tape critical current @77K SF
Tc = 90;                                %[K] critical temperature of HTS tapes
```

```
% operational pressure and temperature ranges
Pop_min_LN2 = 3e5;                      %[Pa] minimal operational pressure allowed for LN2
Pop_max_LN2 = 15e5;                     %[Pa] maximal operational pressure allowed for LN2
Top_min_LN2 = 68;                       %[K] minimal operational temperature allowed for LN2
Top_max_LN2 = 78;                       %[K] maximal operational temperature allowed for LN2
Top_min_HTS = 0;                        %[K] minimal operational temperature allowed for HTS
tapes
Top_max_HTS = Tc;                       %[K] maximal operational temperature allowed for HTS
tapes
```

Intermediate processing

```
% Accounting ofr one-sided cooling configuration
n_cable = n_cable_CA+n_cable_CB;        %[-] nb of cables of system
```

Cable design

```
[cable_architecture]=fct_sc_cable_design(L_cable,Ir,n_cable,DN,former_type,alpha_drill,k_SI,w
_tape,Ic);
```

Pressure drop verification

```
% for CA:
P_in_CA=Pop_max_LN2;
[is_pressure_ok_CA,
P_out_CA]=fct_sc_pressure_verification_hydrodynamic(L_cable,delta_h,DN,mdot,Pop_min_LN2,Pop_m
ax_LN2,P_in_CA);

%for CB mdot doubles
mdot_CB=2*mdot;
[is_pressure_ok_CB,P_out_CB]=fct_sc_pressure_verification_hydrodynamic(L_cable,delta_h,DN,mdo
t_CB,Pop_min_LN2,Pop_max_LN2,P_out_CA);
```

Thermal model

```
thick=cable_architecture.design{:,3}'; % thicknesses of the layers to send to the thermal
model

% Get temperature profiles for cable CA
[T_HTS_AC_CA, T_shield_AC_CA, T_LN2_CA, T_HTS_CA, T_Shield_CA, max_global_temp_CA,
T_out_CA]=fct_cable_thermal_model(T_in,thick,L_cable,sum(cable_architecture.HTSlayer),cable_a
rchitecture.HTSshield,w_tape,mdot,dz);
% verifying temperature restrictions:
is_temperature_ok_CA = fct_cable_tempertaure_verification(T_LN2_CA, T_HTS_CA, T_Shield_CA,
Top_min_LN2,Top_max_LN2,Top_min_HTS,Top_max_HTS);

% Get temperature profiles for cable CB
mdot_out=2*mdot;
```

```
[T_HTS_AC_CB, T_shield_AC_CB, T_LN2_CB, T_HTS_CB, T_Shield_CB ,max_global_temp_CB,
T_out_CB]=fct_cable_thermal_model(T_out_CA,thick,L_cable,sum(cable_architecture.HTSlayer),cab
le_architecture.HTSshield,w_tape,mdot_out,dz);
% verifying temperature restrictions:
is_temperature_ok_CB = fct_cable_tempertaure_verification(T_LN2_CB, T_HTS_CB, T_Shield_CB,
Top_min_LN2,Top_max_LN2,Top_min_HTS,Top_max_HTS);

% Plot Ln2 temperature for repport

% figure();
% Length=[1:2*L_cable/10];
% T_LN2_plot=[T_LN2_CA T_LN2_CB];
% plot(Length,T_LN2_plot);
% grid on
% xlabel('Cable length [m]')
% ylabel('Temperature [K]')
```

AC losses

```
% calculates total AC loses in both the HTS conductor and shield for the
% chosen configuration.

% AC losses for one CA cable:
[AC_loss_cable_CA]=fct_sc_ac_loss(f,Ic,Ir,sum(cable_architecture.HTSlayer),cable_architecture
.HTSshield,T_HTS_AC_CA, T_shield_AC_CA,dz,Tc,T0);

% AC losses for one CB cable:
[AC_loss_cable_CB]=fct_sc_ac_loss(f,Ic,Ir,sum(cable_architecture.HTSlayer),cable_architecture
.HTSshield,T_HTS_AC_CB, T_shield_AC_CB,dz,Tc,T0);

% calculation of total AC losses for the given configuration:
total_AC_losses=AC_loss_cable_CA*n_cable_CA+AC_loss_cable_CB*n_cable_CB;
```

Dielectric losses

```
[dielectric_losses,capacitance,W_dielectric]=fct_sc_dielectric_loss(Vn,f,cable_architecture.d
esign{3,5},cable_architecture.design{4,3},L_cable);

% accounting for number of cables in configuration
total_dielectric_losses = dielectric_losses*n_cable;                    %[W] total
dielectric loss for the configuration
```

Line cryostat losses

```
line_cryo_typical=1.3;                                  %[W/m] typical value for cryostat
termination line according to manufaccturers
line_cryo_cable=fct_sc_line_cryo_loss(line_cryo_typical,L_cable);
total_line_cryo_losses=line_cryo_cable*n_cable;         %[W] line cryostat loss
```

Current lead losses

```
[current_lead_loss_cable]=fct_sc_current_lead_loss(Ir);

% to account for n_cable:
total_current_lead_losses=current_lead_loss_cable*2*n_cable; %[W] total current lead loss for
the configuration
```

Termination Cryostat losses

```
termination_loss=20;                                    %[W] empirical value for losses in on
cryostat termination,load-independent
total_termination_losses=termination_loss*n_cable*2;    %[W] total termination losses
```

Cryocooler Electric consumption

```
req_cooling_capa=total_AC_losses+total_dielectric_losses+total_current_lead_losses+total_term
ination_losses+total_line_cryo_losses;

cryocooler_eff=0.063;                                   %[-] pump efficiency
cryo_elec_consumption=req_cooling_capa/cryocooler_eff;  %[W] total consumption of cryogenic
system
```

Published with MATLAB® R2020b